CHAPTER 11

Catalysis of the Autoxidation of Aquated Sulfur Dioxide by Homogeneous and Heterogeneous Transition Metal Complexes

Scott D. Boyce
Michael R. Hoffman
P. Andrew Hong
Lorraine M. Moberly

GENERAL CONSIDERATIONS

The relationship between acid precipitation and the fate of sulfur dioxide (SO_2) and nitrogen oxides (NO_x) in the atmosphere has become the subject of intensive study in recent years. Fundamental questions about the multifarious pathways for the chemical transformation of SO_2 and NO_x to oxyacids remain to be answered before a complete description of this complex reaction network can be provided.

SO_2 and NO_x can be oxidized to acidic sulfate and nitrate aerosols either homogeneously in the gas phase or heterogeneously in atmospheric microdroplets [1–3]. Field studies indicate that the relative importance of homogeneous and heterogeneous processes depends on a variety of climatological factors such as relative humidity and the intensity of incident solar radiation [4–9].

Until recently, most literature discussions of the oxidation of SO_2 have focused on homogeneous gas-phase reactions involving hydroxyl ($HO\cdot$) and hydroperoxyl ($HO_2\cdot$) radicals. However, recent measurements have indicated that the rates of oxidation of SO_2 by $HO_2\cdot$ and organic peroxides are slower than previously thought [1]. Furthermore, the apparent oxidation rate of sulfur dioxide by $HO\cdot$ also does not appear to be sufficiently fast to account for observed sulfate formation rates in the atmosphere [2,3]. This is especially true in cases where rapid conversion of SO_2 has been observed under conditions of high humidity or at night in the

absence of photolytically generated radical species [4]. For these reasons, it is now believed that condensed-phase (i.e., aqueous solution) homogeneous and heterogeneous pathways contribute significantly to the production of sulfuric acid (H_2SO_4) in the atmospheric microdroplets. As a result, considerable experimental and theoretical work has been directed toward an evaluation of the potential role of ozone (O_3), hydrogen peroxide (H_2O_2) and nitrous acid (HNO_2) as liquid-phase oxidants. The reactions of SO_2 with these species in aqueous solution are discussed by Schwartz [10] and Martin [11].

Catalytic autoxidation of sulfur dioxide dissolved in aqueous microdroplets has been suggested as a nonphotolytic pathway for the rapid accumulation of sulfuric acid in humid atmospheres [12–20]. In general, reactions of the triplet ground electronic state of molecular oxygen (O_2) (Figure 1) with singlet state reductants such as SO_2 proceed slowly because they involve changes in spin multiplicity and a large degree of bond deformation or alteration in the formation of products. In many cases, autoxidation reactions can be initiated photolytically through irradiation of the reactant species. For example, ultraviolet light exerts a strong catalytic effect on the solution-phase autoxidation of SO_2 [21]. Alternatively, the reactions of O_2 with a variety of organic and inorganic substrates can be accelerated in the presence of transition metal ions, such as Co(II), Co(III), Cu(II), Fe(II), Fe(III), Mn(II) and Ni(II) [22,23].

Oxidation of sulfur dioxide by molecular oxygen proceeds according to the following stoichiometry:

$$S(IV) + \frac{1}{2} O_2 \longrightarrow H_2SO_4 \qquad (1)$$

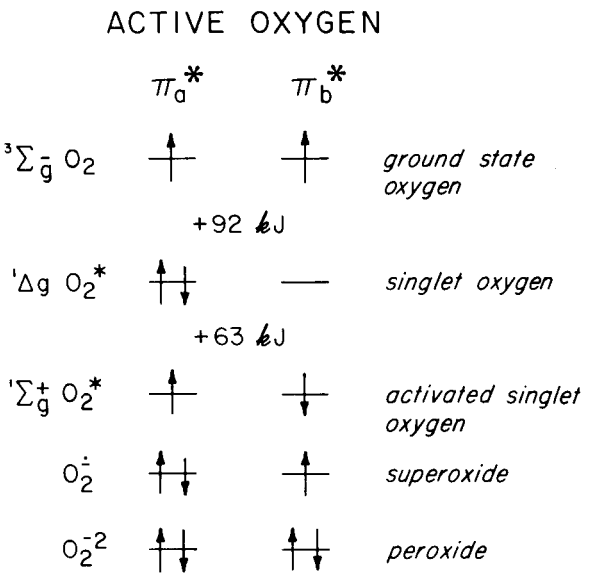

Figure 1. Electronic distributions into pi-antibonding orbitals of dioxygen according to molecular orbital theory and associated energies shown with corresponding spin states.

S(IV) denotes the overall speciation of SO_2 in aqueous solution including aquated sulfur dioxide ($SO_2 \cdot H_2O$), bisulfite ion (HSO_3^-) and sulfite ion (SO_3^{2-}) such that $[S(IV)] \simeq [SO_2 \cdot H_2O] + [HSO_3^-] + [SO_3^{2-}]$. This reaction is particularly sensitive to catalysis by metal ions at trace concentrations. Numerous investigators have examined the kinetics of this redox process under a wide range of experimental conditions [16,24–35]. Unfortunately, the results of these studies (Table I) show a considerable degree of disagreement as to the quantitative effects of catalyst (metal ion) concentration, pH and light on the rate of autoxidation.

A review of the available literature [36] revealed that three general categories of mechanistic pathways have been proposed to explain observed kinetic data. The postulated mechanisms include:

1. Thermally initiated free-radical chain processes involving a sequence of one-electron transfer steps such as [37]:

initiation: $$M^{n+} + SO_3^{2-} \longrightarrow M^{(n-1)+} + SO_3^{-} \quad (2)$$

propagation: $$SO_3^{-} + O_2 \longrightarrow SO_5^{-} \quad (3)$$

$$SO_5^{-} + SO_3^{2-} \longrightarrow SO_5^{2-} + SO_3^{-} \quad (4)$$

oxidation: $$SO_5^{2-} + SO_3^{2-} \longrightarrow 2SO_4^{2-} \quad (5)$$

termination: $$2SO_3^{-} \longrightarrow S_2O_6^{2-} \quad (6)$$

$$SO_3^{-} + SO_5^{-} \longrightarrow S_2O_6^{2-} + O_2 \quad (7)$$

$$2SO_5^{-} \longrightarrow S_2O_6^{2-} + 2O_2 \quad (8)$$

Table I. Empirical Rate Laws Reported for Metal-Catalyzed Autoxidation of SO_2^a

M^{n+}				*Reference*
Fe^{3+}	1	1–2	?	16
	1	1	0	26,28
Cu^{2+}	0.5	1.5	0	24
	1	1	0	31
Co^{2+}	0.5	1.5	0	25
	2	1	1	29
	0.5	?	1	32
	1	1	1	35
Co^{3+}	0.5	1.5	0	27
	0.5	?	2	34
Mn^{2+}	2	0	0	28
	≤1	≤1	0	33

2. Nonradical, polar mechanisms in which formation of an inner-sphere metal sulfite coordination complex precedes two-electron transfer from the substrate to oxygen [30,38]:

$$M^{n+} + SO_3^{2-} \rightleftharpoons MSO_3^{(n-2)+} \tag{9}$$

$$MSO_3^{(n-2)+} + SO_3^{2-} \rightleftharpoons M(SO_3)_2^{(n-4)+} \tag{10}$$

$$M(SO_3)_2^{(n-4)+} + O_2 \rightleftharpoons M(SO_3)_2\ O_2^{(n-4)+} \tag{11}$$

$$M(SO_3)_2 \cdot O_2^{(n-4)+} \xrightarrow[\text{slow}]{} M^{n+} + 2SO_4^{2-} \tag{12}$$

3. Photoassisted pathways in which the reaction is initiated through absorption of light ($h\nu$) by sulfite, the metal ion or a metal-sulfite complex [39]:

Of the three alternatives, free-radical mechanisms are most frequently cited in attempts to achieve an adequate interpretation of experimental measurements. Several modifications to the scheme originally suggested by Backström [37] (Equations 2–8) have also been reported in which species such as the sulfate radical ($SO_4^{\cdot-}$), $HO_2\cdot$ and $HO\cdot$ are thought to act as chain carriers [21,40]. From an analysis of kinetic expressions corresponding to the various hypothetical mechanisms, it became apparent that the kinetics of the autoxidation of sulfite conform to a complex multiterm rate law.

The basic hypothesis that governs the research being conducted in the authors' laboratory is that the autoxidation of aquated SO_2 and other water-soluble reductants and the nonphotolytic production of H_2O_2, $HO_2\cdot$ and $HO\cdot$ as liquid-phase oxidants may represent interrelated phenomena. According to this scheme, hydrogen peroxide would form as a two-electron reduction product of O_2 from a catalyzed reaction pathway in which molecular oxygen is "activated" via coordination to a transition metal center. Complexation of dioxygen reduces the activation energy barrier for direct reaction of O_2 with a substrate. It is well understood that numerous metalloenzyme redox systems function in this manner [41]. Subsequently, H_2O_2 may either decompose in the presence of metal ions such as iron to form hydroxyl and hydroperoxyl radical intermediates as in the classic "Fenton's reagent" cycle [42]:

$$Fe^{2+} + H_2O_2 \longrightarrow Fe(OH)^{2+} + HO\cdot \tag{13}$$

$$Fe^{3+} + H_2O_2 \longrightarrow Fe^{2+} + H^+ + HO_2\cdot \tag{14}$$

$$Fe^{3+} + HO_2\cdot \longrightarrow Fe^{2+} + H^+ + O_2 \tag{15}$$

$$HO\cdot + H_2O_2 \longrightarrow H_2O + HO_2\cdot \tag{16}$$

$$HO_2\cdot + H_2O_2 \longrightarrow O_2 + H_2O + HO\cdot \qquad (17)$$

or participate directly in the oxidation of additional dissolved sulfur dioxide.

EXPERIMENTAL OBJECTIVES

To investigate further some of the fundamental aspects of the solution-phase oxidation of sulfur dioxide, a study of the reaction of dissolved SO_2 with molecular oxygen in a well defined catalytic system was undertaken. In natural systems, transition-metal ions are frequently associated with organic and inorganic ligands. Lunde et al. [43] have identified a broad range of organic micropollutants, including several aliphatic and aromatic carboxylic acids in precipitation samples collected over Norway. Many of these compounds could readily form stable coordination complexes with trace metal species dissolved in atmospheric microdroplets. Unfortunately, only a very few studies of the catalytic properties of organometallic complexes have been carried out using aqueous solutions.

One type of organometallic complex that has been the subject of detailed examination is the phthalocyanine series. Phthalocyanines are tetrapyrrole derivatives that form square planar complexes in which a divalent metal ion, M(II) is coordinated to the four pyrrole nitrogen atoms of the macrocyclic structure as depicted in Figure 2. Metal-phthalocyanines have been shown to be effective homo-

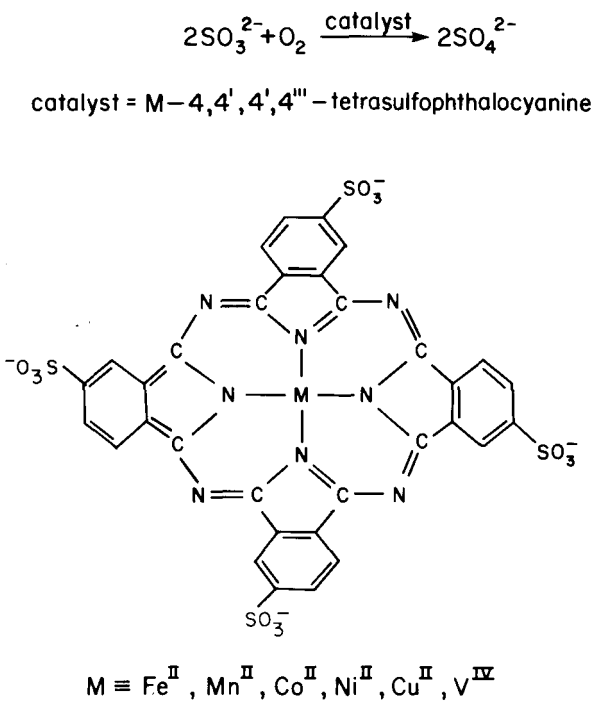

Figure 2. Stoichiometric relationship between sulfite and sulfate in metal-catalyzed reactions where the stoichiometric coefficient for oxygen is 0.5 and the catalyst is Co(II).

geneous and heterogeneous catalysts for the autoxidation of many types of substrates, including aldehydes [44,45], phenols [46,47], mercaptans [48], hydrazine [49], and hydroxylamine [50].

Hoffmann and Lim [51] have studied the catalyzed autoxidation of hydrogen sulfide (HS^-) in aqueous solution over the pH range 5–12. The catalytic properties of water-soluble Co(II)-, Cu(II)- and Ni(II)-4,4′,4″,4′″-tetrasulfophthalocyanines (M(II)-TSP) were evaluated in terms of the generalized rate equation:

$$\nu = \frac{-d[HS^-]}{dt} = \frac{k[M(II)TSP][O_2][HS^-]}{K_C + K_B + K_A[HS^-] + [O_2][HS^-]} \tag{18}$$

which simplifies to a rate law with an apparent zero-order dependence on $[O_2]$ and first-order dependence on $[HS^-]$ when $[O_2] >> [HS^-] > K_C$ and $K_B > [HS^-]$.

$$\nu = k'[M(II)TSP][HS^-] \tag{19}$$

Mechanistically, the kinetic expression of Equation 18 combined with spectrophotometric data indicate that the reaction proceeds via the formation of a ternary activated complex in which O_2 and HS^- are reversibly bound to the metal center as shown below for Co(II)-TSP:

$$Co(II)TSP + O_2 \overset{\beta_1}{\rightleftharpoons} Co(III)TSP\text{-}O_2\cdot \tag{20}$$

$$Co(III)TSP\cdot O_2 + HS^{2-} \overset{\beta_2}{\rightleftharpoons} Co(III)TSP\text{-}O_2\cdot SH^- \tag{21}$$

$$Co(III)TSP\text{-}O_2\cdot SH^- \xrightarrow[\text{slow}]{k} Co(II)TSP + HSO_2^- \tag{22}$$

$$HSO_2^- + O_2 \rightleftharpoons HSO_4^- \tag{23}$$

$$Co(III)TSP\text{-}O_2\cdot SH^- \rightleftharpoons Co(II)TSP\text{-}O_2H^- + S^o \tag{24}$$

$$Co(II)TSP\text{-}O_2H^- + H^+ \rightleftharpoons Co(II)TSP + H_2O_2 \tag{25}$$

$$H_2O_2 + S^o \longrightarrow H_2SO_2 \xrightarrow{O_2} H_2SO_4 \tag{26}$$

The terms K_A, K_B and K_C in the overall kinetic expression for this process (Equation 18) correspond to collections of the forward and reverse rate constants for the individual complexation reactions (Equations 20 and 21) that precede the rate-controlling step. Redox processes that are sensitive to homogeneous trace metal catalysis often exhibit rate laws that are first order with respect to the concentration of reductant and zero order in oxidant. Experimental results suggested that the autoxidation of dissolved SO_2 also falls into this general category of redox reactions.

This chapter describes the synthesis of both water-soluble metal phthalocyanine derivatives and their solid-supported analogs, which were formed by attachment of the macrocyclic complex to an inert silica gel surface. These compounds were subsequently used as active homogeneous and heterogeneous catalysts for the autoxidation of aquated SO_2 due to their well defined geometry and chemical behavior in aqueous media. Certain metal-phthalocyanines such as Co(II)-TSP are known to actively bind dioxygen and serve as O_2 carriers in solution [52].

Preliminary kinetic measurements and mechanistic results are described in this chapter. Particular emphasis is focused on the following features of the catalytic process:

1. Alternatives of one- or two-electron transfer steps;
2. Binding of molecular oxygen by an active catalytic center;
3. Inner-sphere complexation of the substrate as a prelude to electron transfer;
4. The possible role of photoassisted metal catalysis, and
5. Changes in catalytic behavior when the metal complex is anchored to a solid surface.

EXPERIMENTAL PROCEDURE

Synthesis of Co(II)-Phthalocyanine Complexes

Co(II)-4,4′,4″,4′″-tetraminophalocyanine [Co(II)-TAP] was prepared according to a procedure derived from the method of Weber and Busch [53]. A mixture of 4-aminophthalic acid, ammonium molybdate, ammonium chloride and Co(II) sulfate-7-hydrate was heated under reflux in nitrobenzene for 6 h. The crude product was washed with methanol and subsequently heated to boiling in 0.5 *M* HCl. After filtration, dissolution in dimethylsulfoxide (DMSO) at 70 C removed the insoluble impurities. The product crystallized on addition of (500 mL) H_2O and was isolated by centrifugation. Further purification involved repetitive washings of the solid in boiling H_2O and centrifugation. After initial treatment with absolute ethanol, pure Co(II)-TAP was obtained by heating the solid in absolute ethanol under reflux for 5 h. The tetrasodium salt of Co(II)-4,4′,4″,4′″-tetrasulfophothalocyanine was synthesized in an analogous manner. The structure of each complex was confirmed by elemental analysis (Table II), ultraviolet/visible (UV/VIS) and ^{1}H nuclear magnetic resonance (NMR) spectrophotometry.

Preparation of the Heterogeneous Catalyst Support

Preparation of the catalyst supported involved the treatment of silica gel with an appropriate silylation reagent as illustrated in Figure 3 [54,55]. In preparation I, a suspension of 22 g of silica gel (Fisher Scientific, specific area 330 $m^2 g^{-1}$) and

Table II. Elemental Analyses of Co(II)-Phthalocyanine Complexes[a]

	Co(II)-TSPc		*Co(II)-TAPc*	
	Calculated	*Found*	*Calculated*	*Found*
% C	37.82	36.95	57.48	49.83
% H	1.59	2.03	3.40	3.88
% N	11.04	10.73	25.19	23.07
% S	12.63	12.12		

[a] Elemental analyses performed by Galbraith Laboratories, Inc., Knoxville, Tennessee.

7.5 g of 3-chloropropyltrimethoxysilane in 150 mL xylene was heated under reflux for 8 h. Addition of 3.5 g of imidazole enabled the formation of product II. After filtration, the modified gel was washed with acetone and allowed to dry in the atmosphere overnight. Gel II contained 1.71×10^{-3} mol-g^{-1} of nitrogen as determined by elemental analysis.

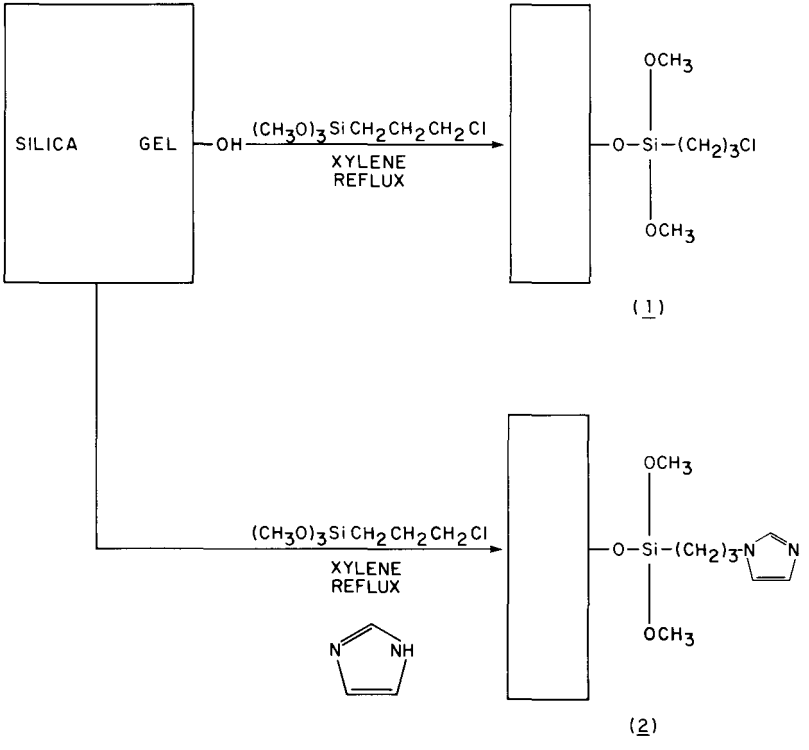

Figure 3. Flow diagram for the preparation of a modified silica gel system for Co(II)-TAP and Co(II)-TSP catalysts using 3-chloropropyltrimethoxysilane and imidazole as reagents.

Attachment of Co(II) Phthalocyanine Complexes to the Solid Support

Two methods were used to anchor the Co(II) phthalocyanine complexes to the modified silica gel. In scheme 1 (Figure 4), attachment was achieved through covalent bonding of the surface ligand to the amino side chain of Co(II)-TAP. The second procedure (scheme 2) involved direct complexation of the modified silica gel surface to the central metal atom of the phthalocyanine complexes.

Scheme 1

A stirred mixture of the modified silica gel and 6.7 g Co(II)-TAP in 30 mL DMSO was heated at 80 C for 4 h. The hybrid catalyst was isolated by filtration and washed successively with warm DMSO and 0.1 *M* NaOH to remove any residual chloride. Final purification was attained by extraction of the product with H_2O in a Soxhlet apparatus for 5 h. The supported Co(II)-TAP III was dried in an oven at 80 C. Elemental analysis revealed 2.7×10^{-5} mol-g^{-1} of Co (0.16%).

Scheme 2

In this procedure, a 2.5-cm-diameter column was packed with modified gel. A 150-mL volume of a 7.8×10^{-5} *M* aqueous Co(II)-TSP solution was poured into the column and eluted dropwise. DMSO was used as a solvent for Co(II)-TAP. The hybrid products IV and V were washed several times with the appropriate solvent and collected by filtration. Analysis of the eluent from the column by UV/VIS spectrophotometry indicated the following Co(II) content for each supported catalyst:

- Co(II)-TSP: 1.09×10^{-6} moles of Co per gram of solid, and
- Co(II)-TAP: 1.19×10^{-6} moles of Co per gram of solid.

Kinetic Measurements

Reagents

Sulfite solutions were prepared from reagent-grade Na_2SO_3 (Mallinkrodt). The following reagent-grade chemicals were used to prepare the pH buffer solutions:

- tris-(hydroxymethyl) aminomethane (TRIS), Sigma;
- tris-(hydroxymethyl) aminomethane hydrochloride (TRIS-HCl), Sigma;
- N-tris-(hydroxymethyl) methyl-2-aminomethane sulfonic acid (TES), Sigma;
- sodium phosphate—monobasic, Mallinkrodt;
- sodium phosphate—dibasic, Mallinkrodt;
- sodium phosphate—tribasic, Mallinkrodt;
- sodium borate, Mallinkrodt;

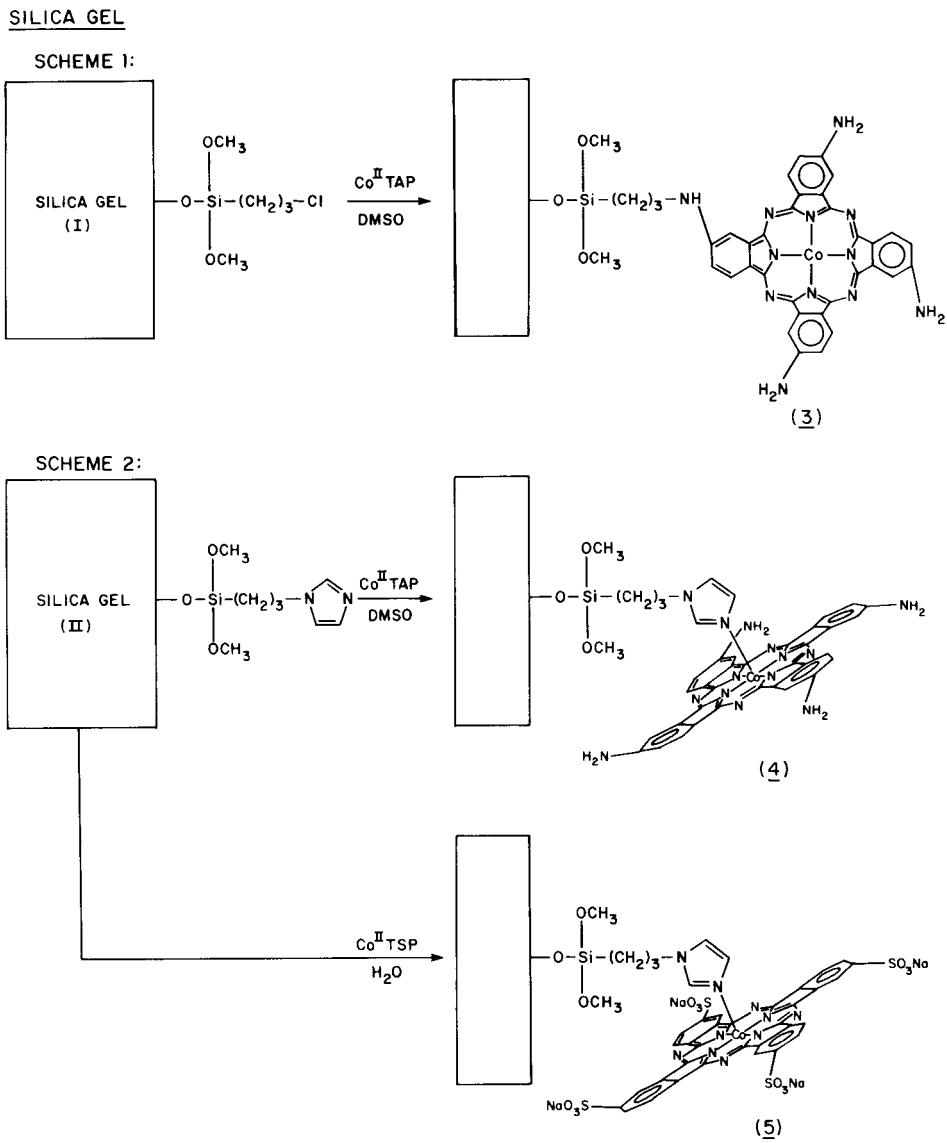

Figure 4. Modes of attachment of cobalt phthalocyanine complexes to silica gel support systems I and II. Attachment was achieved by indirect linkage through a ring amino group (III) and by direct coordination through the central metal of the complex (IV and V).

- sodium chloride, Mallinkrodt; and
- sodium hydroxide, Mallinkrodt.

Sodium perchlorate (G. F. Smith) was used to maintain the ionic strength constant at $\mu = 0.4$ *M*. Deionized water (18 MΩ-cm resistivity) obtained from a Milli RO-4/Milli Q purification system (Millipore) was used in the preparation of all reagent solutions. The water was deoxygenated by purging with N_2 before preparation of the Na_2SO_3 solutions.

Kinetic Data

Kinetic data were obtained from two series of experiments. In the initial set of experiments with the homogeneous Co(II)-TSP catalyst, sulfite concentration [S(IV)] was determined by monitoring the UV absorption spectrum ($\lambda_{max} = 212$ nm) of the reaction solution as a function of time. Optical absorption data were collected with a Hewlett-Packard Model 8450A UV/VIS spectrophotometer. The instrument was equipped with a reversed-optic diode detector, which permitted simultaneous detection over 200–800 nm in 1 s. As a result, changes in the absorption spectrum of Co(II)-TSP were also recorded during the reaction. The reactions were performed at 24 ± 1 C directly in Teflon-stoppered quartz spectrophotometer cells (2 or 10 cm pathlength).

In a second set of experiments, the reactions were followed by continuous measurement of O_2 concentration as a function of time. Dissolved oxygen was determined using an Orion Model 97–08–00 O_2 electrode coupled to an Orion Model 901 Ionanalyzer/Model 951 digital printer system. The pH of the reaction mixture was monitored simultaneously via an Orion combination pH electrode. The O_2 and pH electrodes were interfaced to the Ionanalyzer through an Orion Model 605 Electrode Switch.

These reactions were conducted in a water-jacketed glass and Teflon reactor with a total volume of 2.0 L. The design and operation of the batch reactor has been described previously [51]. To minimize the potential catalytic effect of trace metal contaminants, all glassware was washed with phosphate-free detergent (Alconox), soaked in 5.2 *M* HNO_3, and rinsed several times with deionized water.

In a typical experiment, a 2.0-L volume of a buffer solution and the appropriate catalyst were transferred to the reactor system. Air (Matheson), oxygen (Matheson) or a controlled N_2/O_2 mixture was purged through the solution with constant stirring for 30 min. After saturation, the reactor was sealed from the atmosphere. A constant temperature of 25 ± 0.1 C was maintained using a Haake Model FK-2 water circulation system and temperature controller.

To initiate a reaction, a known volume of a stock sulfite solution was added to the buffer-catalyst mixture. [S(IV)] ranged from 5×10^{-5} to 5×10^{-3} *M*. Dissolved oxygen varied from 2.5×10^{-4} to 1.2×10^{-3} *M*. Addition of ethylenediaminetetracetic acid (EDTA) disodium salt (Sigma) reduced the catalytic effect of residual trace metal contaminants in control reactions [58]. Mannitol, sodium cyanide (NaCN) and EDTA were used selectively as free radical scavengers [37] and trace metal complexation inhibitors [57].

RESULTS AND DISCUSSION

Homogeneous Catalysis by Co(II)-, Fe(II)-, Mn(II)-, Ni(II)-, Cu(II)- and V(IV)-4,4',4'',4'''-Tetrasulfophthalocyanine Complexes

Reaction Rate as a Function of Total Sulfite Concentration

The catalytic rate for the oxidation of S(IV) by oxygen was followed spectrophotometrically as described in the experimental section. Reactions were conducted under pseudo-first-order conditions in sulfite at constant pH and ionic strength (i.e., $[O_2]_o >> [S(IV)]_o$ where $[S(IV)] \simeq [HSO_3^-] + [SO_3^{2-}]$ at pH > 3.0). The observed rate constants (k_{obs}) for the reactions were calculated from plots of absorbance ($ln A_t/A_o$) vs time.

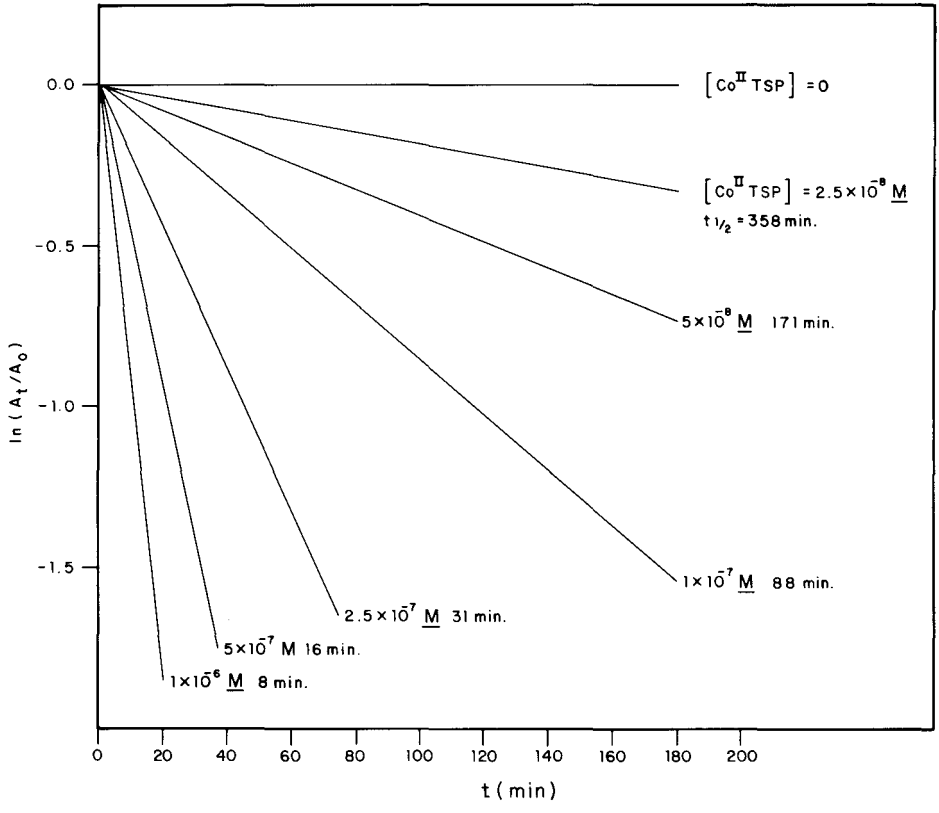

Figure 5. Pseudo-first-order plots of $ln(A_t/A_o)$ for the reaction of S(IV) with O_2 at pH 9.2 in a borate buffer system with $\mu = 0.4$.

Kinetic data obtained from a typical series of experiments are summarized in Figure 5. At the principal wavelength for light absorption due to SO_3^{2-} (λ_{max} = 212 nm), Beer's law ($A = \epsilon lc$) was valid over a broad range of [S(IV)] as reported previously [21]. Under the reaction conditions outlined in Figure 5, the observed pseudo-first-order rate constants ranged from 3.35×10^{-5} s^{-1} at $[Co(II)\text{-}TSP]_o = 2.5 \times 10^{-8}$ M to 5.21×10^{-3} s^{-1} at $[Co(II)\text{-}TSP]_o = 2.5 \times 10^{-6}$ M ($0.985 < R^2 < 0.999$) under alkaline conditions (pH 9.2). No measurable decrease in [S(IV)] was detected after 12 h in the absence of Co(II)-TSP.

Similar first-order behavior in total sulfite was observed in neutral solution (pH 6.7) and over the entire pH range under study. The linearity of plots of $ln\ A_t/A_o$ as a function of time can be accepted as conclusive evidence that the reaction order in [S(IV)] is unity. Further support for this conclusion is provided by the kinetic results collected from the measurement of changes in the concentration of dissolved oxygen during the course of the reaction. The amperometric response of the oxygen electrode is a linear function of the aqueous-phase O_2 concentration ($i_\infty \alpha [O_2]$). A plot of electrode response vs time was linear from t = O for experiments conducted under initial reaction conditions in which $[O_2]_o >> [S(IV)]_o$.

Application of the van't Hoff method of initial rates to the results determined from $[O_2]$ vs time functions enabled us to calculate the reaction order in total sulfite over a wide range in [S(IV)]. Shown in Figure 6 are *ln-ln* plots of the initial rate of oxygen depletion ($\nu_o = -d[O_2]_o/dt$) as a function of $[S(IV)]_o$ for a series of reactions performed at pH 6.7 and 9.2. The slopes of these linear functions (1.18 at pH 6.7 and 1.25 at pH 9.2) confirm that the reaction order in [S(IV)] is approximately one. A moderate degree of uncertainty in the experimental measurements accounts for the empirical values of slightly greater than unity. This observation suggests that one source of variability in reaction orders previously reported for the metal-catalyzed autoxidation of dissolved SO_2 (Table I) may be due to selective fitting of experimental results over a narrow concentration range and/or a moderate degree of scatter in data points.

Reaction Rate as a Function of Total Oxygen Concentration

The dissolved oxygen vs time profiles exhibited zero-order behavior throughout most of the reactant concentration ranges employed in the kinetic evaluations. However, deviations from linearity were observed when the initial concentration conditions were designed such that $[S(IV)]_o >> [O_2]_o$. Under these circumstances, an apparent exponential decay in the concentration of oxygen as a function of time was detected. The latter result signifies either the attainment of a "saturation effect" as would be predicted for enzymatic catalysis or a shift in the reaction mechanism with a change in relative reactant concentrations.

Additional evidence for a rate law bearing a zero-order dependence in $[O_2]$ was obtained through the determination of k_{obs} at different initial concentrations of dissolved oxygen. The observed first order kinetic constants that were measured over a range of $[O_2]_o$ from 2.5×10^{-4} to 1.2×10^{-3} M remained constant within

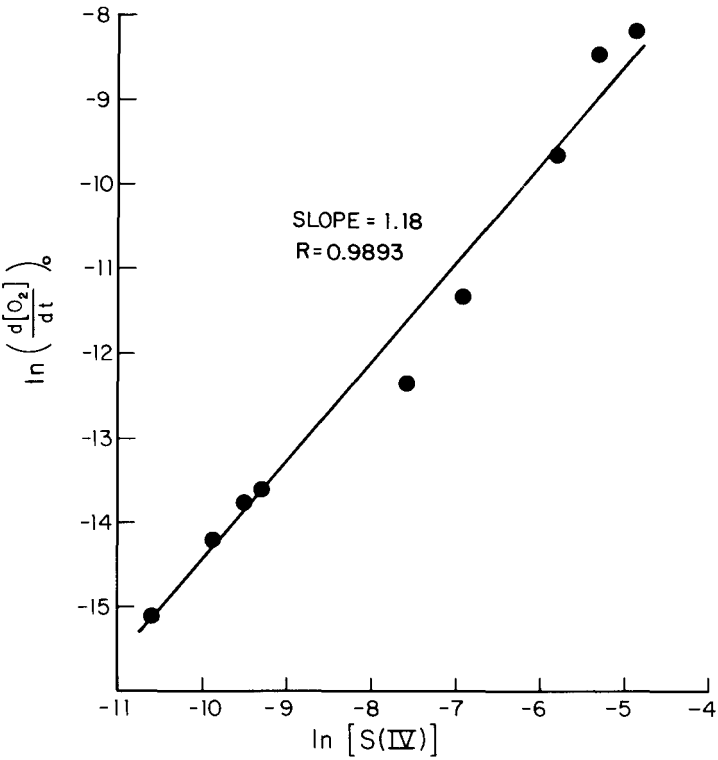

Figure 6. Determination of the S(IV) reaction order by the van't Hoff method of initial rates where $d[O_2]/dt$ is obtained from the slope of $[O_2]$ vs time response function at $t = 0$.

the limits of experimental error (±5%) under both neutral and alkaline pH conditions.

Reaction Rate as a Function of Total Catalyst Concentration

The experimental data presented in Figure 5 were examined to determine the influence of catalyst concentration as the observed rate of sulfite oxidation. A plot of *ln* k_{obs} vs *ln* $[Co(II)TSP]_o$ indicates that the reaction order with respect to cobalt-phthalocyanine is approximately 1.0 at pH 9.2 (Figure 7a). However, a comparable analysis of kinetic measurements recorded from reactions conducted in neutral solution yields a nonintegral concentration dependence of 0.3 (Figure 7b). This variability in reaction order implies that a change in the catalyzed autoxidation mechanism may accompany a change in the pH of the reaction solution. Alternatively, an increase in pH could affect the speciation of active forms of

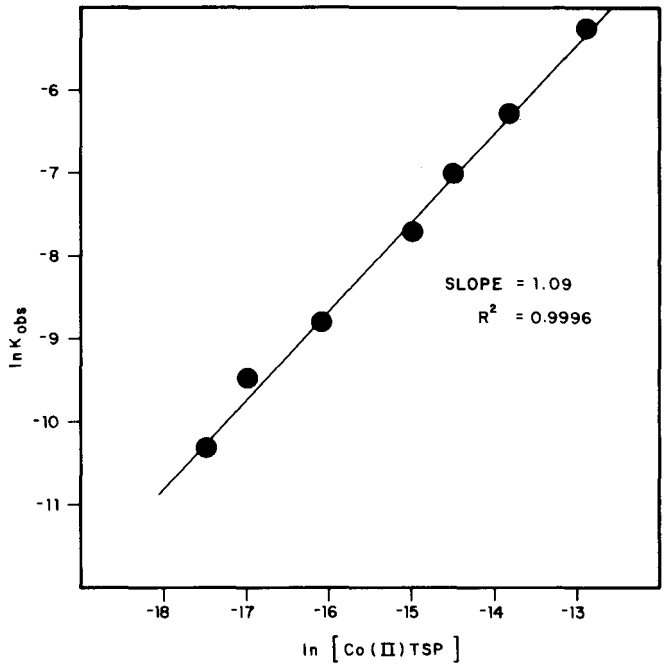

(a)

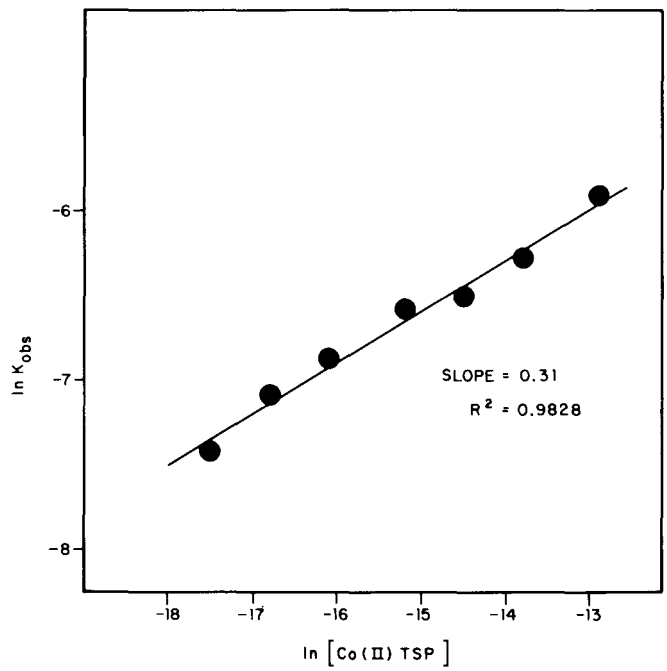

(b)

Figure 7. Determination of the reaction order with respect to the total concentration at pH 9.2 (a) and pH 6.7 (b).

the catalyst through a shift in the equilibria between monomeric and polymeric structures of the Co(II)-TSP complex.

Ancillary Observations: Effects of pH, Complexation, Inhibitors, Light and Central Metal Atom on Reaction Rate

Since this report constitutes a preliminary communication, exhaustive parametric results will not be presented; however, sufficient information is available at this stage to formulate tentative conclusions about many of the primary and secondary factors affecting the autoxidation rate of aquated sulfur dioxide.

The pH-dependence of the oxidation of sulfite by molecular oxygen is unusually complicated as shown in Table III. The sharp increase in the catalyzed reaction rate between pH 4.1 and 6.7 may be attributed to the acid dissociation of bisulfite to give sulfite ion:

$$HSO_3^- \underset{K_a}{\rightleftharpoons} H^+ + SO_3^{2-} \tag{27}$$

$K_a = 1.62 \times 10^{-7}$ *M* ($pK_a = 6.79$) at a temperature of 20 C and ionic strength $\mu = 0.1$ *M* [56]. As the fraction of [S(IV)] present at SO_3^{2-} increases, the rate of autoxidation also increases. This behavior clearly shows that sulfite is the principal reactive S(IV) species in aqueous solution.

As suggested previously [30,33,38], the rate-controlling step in the catalyzed autoxidation of dissolved SO_2 is preceded by rapid formation of discrete inner-sphere complexes between the active metal center and sulfite. While numerous investigators have successfully characterized the structure of crystalline metal-sulfite salts [58–64] few stability constants and rate constants have been reported for the formation of these species in solution due to the instability of SO_3^{2-} toward oxidation. However, it is interesting to note that the thermodynamic constants which have been reported are significantly larger than corresponding β values for metal-sulfate derivatives (Table IV).

Table III. Effect of pH on v_o: Results of pH Dependence Study[a]

pH	*Buffer System*	v_o (10^3 *M-min*$^{-1}$)
4.4	0.1 *M* NaH_2PO_4; 0.3 *M* $NaClO_4$	No reaction
6.9	0.1 *M* NaH_2PO_4; 0.1 *M* Na_2HPO_4	-7.6856×10^{-7}
7.7	0.2 *M* TES; 0.1 *M* NaOH; 0.3 *M* $NaClO_4$	-9.675×10^{-8}
8.4	0.1 *M* TRIS; 0.1 *M* TRIS-HCl; 0.3 *M* $NaClO_4$	-1.355×10^{-7}
9.4	0.1 *M* NaB_4O_7; 0.1 *M* $NaClO_4$	-1.581×10^{-6}
10.1	0.1 *M* Na_2CO_3; 0.1 *M* $NaHCO_3$	-1.041×10^{-6}
11.5	0.044 *M* Na_2HPO_4; 0.444 *M* Na_3PO_4	-1.256×10^{-6}
12.7	0.1 *M* NaCl; 0.1 *M* NaOH; 0.2 *M* $NaClO_4$	-2.1053×10^{-6}

Table IV. Comparison of Stability Constants[a] for Metal-Sulfito and -Sulfato Complexes at 25.0 C

Metal	μ	*log* β, SO_3^{2-}	μ	*log* β, SO_4^{2-}
Ag^+	0	$AgSO_3^+$, 5.6	0	$AgSO_4^+$, 1.3
Cd^{2+}	1.0	$Cd(SO_3)_2^{2-}$, 4.2	1.0	$Cd(SO_4)_2^{2-}$, 1.6
Hg^{2+}	1.0	$Hg(SO_3)_2^{2-}$, 24.1	0.5	$Hg(SO_4)_2^{2-}$, 2.4
Ce^{3+}	0	$CdSO_3^+$, 8.0	0	$CdSO_4^+$, 3.6
Fe^{3+}	0.1	$FeSO_3^+$, 18.1[b]	0	$FeSO_4^+$, 4.0
Fe^{2+}			0	$FeSO_4^0$, 2.2

[a] All constants reported in this table were taken from Smith and Martell [57], except that for $FeSO_3^+$.
[b] Hansen et al. [65].

$$Fe^{3+} + H_2O \cdot SO_2 \rightleftharpoons FeSO_3^+ + 2H^+ \qquad \log K = 9.7$$
$$H^+ + HSO_3^- \rightleftharpoons H_2O \cdot SO_2 \qquad \log K = 1.6$$
$$H^+ + SO_3^{2-} \rightleftharpoons HSO_3^- \qquad \log K = 6.8$$
$$Fe^{3+} + SO_3^{2-} \rightleftharpoons FeSO_3^+ \qquad \log K = 18.1$$

Carlyle [66] has reported that evidence for inner-sphere complexation of Fe(III) and subsequent reduction by coordinated sulfite can be observed visually: "iron(III) solutions became brown-red upon addition of sulfite and then slowly fade." Similar changes in color have also been described by Hoffmann et al. [66] for the oxidation of vanadyl cation (VO^{2+}) by peroxydiphosphate ($H_2P_2O_8^{2-}$). For this redox system, kinetic measurements showed that formation of an inner-sphere complex of finite stability ($\log \beta \simeq 4.0$) occurred before electron transfer, which took place on a slower time scale.

Preliminary experimental evidence that sulfite and/or dioxygen coordination play an important role in the phthalocyanine-catalyzed reactions was obtained through the introduction of competitive complexing reagents. Addition of EDTA and cyanide to reaction solutions containing Co(II)-TSP resulted in a significant reduction in k_{obs} at pH 9.2, whereas only EDTA exerted a negative influence on the reaction rate at pH 6.7 (Table V). Under neutral pH conditions, the inhibitory effect of EDTA appears to be associated primarily with the complexation of background levels of trace-metal contaminants. For example, the half-life for the uncatalyzed oxidation of sulfite in the absence of EDTA increased from 333 to ~1800 min at an EDTA concentration of 10^{-5} *M*. In neutral solution, cyanide failed to inhibit the reaction because it exists almost completely as HCN ($pK_a = 9.2$), which is a much weaker ligand than CN^- for the binding of transition metal ions [57]. However, the oxidation of sulfite ceased completely at pH 11.5 on addition of sodium cyanide at 10^{-5} *M* concentrations. In contrast, reactions conducted in the presence of an equivalent concentration of an effective free-radical inhibitor (d-mannitol at 10^{-5} *M*) were retarded only to a slight degree.

Direct spectrophotometric evidence for the complexation of sulfite and O_2

Table V. Effect of Inhibitors on k_{obs} at pH 6.7 and 9.2[a]

Inhibitor	*Inhibitor Concentration* (10^6 *M*)	k_{obs} (10^3 s^{-1}) *pH 6.7*	*pH 9.4*
None	0	1.62	1.83
EDTA	1	1.52	
	2.5	1.45	
	5.0	0.94	
	10.0	0.78	0.33
Mannitol	10.0	1.25	0.85
NaCN	10.0	1.61	0.29

[a] Initial conditions: $[S(IV)]_o = 10^{-4}$ *M*; $[O_2]_o = 10^{-3}$ *M*; $[Co(II)\text{-}TSP]_o = 10^{-6}$ *M*; $\mu = 0.4$; T = 26.0 C.

by cobalt-phthalocyanine has been obtained as shown in Figure 8. The visible spectrum of Co(II)-TSP, denoted by the solid line in Figure 8, has two characteristic absorption bands, which have been attributed to an oxygen-free monomer complex (λ_{max} = 636 nm) and to a monomeric dioxygen adduct (λ_{max} = 670 nm) [68,69]. Other researchers [70–72] have interpreted these spectral characteristics in terms of a simple monomer/dimer equilibrium, in which the electronic transition at higher energy is associated with the dimeric phthalocyanine complex. Hoffmann and Lim [51] observed that the absorbance of the peak at 670 nm increased on dissolution of Co(II)-TSP in progressively more alkaline solutions containing O_2. Over the pH range 9–12, this behavior was accompanied by a decrease in the value of A_{636}.

At the beginning of a typical autoxidation reaction, the spectrum of the catalyst changes dramatically on addition of sulfite, as indicated by the dotted line in Figure 8. Introduction of sulfite causes a rapid growth of the absorption maximum at 670 nm in relative proportion to the peak at 636 nm. The value of A_{670} decreases slowly with time as the oxidation reaction proceeds. At the conclusion of the reaction, the absorbance at 670 nm is comparable to the initial intensity of the 636-nm peak as represented by the dashed-line spectrum. Further addition of sulfite results in the reemergence and subsequent decline of the peak at λ_{max} = 670 nm as the second catalytic cycle unfolds. This spectroscopic behavior can be reproduced a number of times with slight changes in catalytic activity as indicated by the tabulation of observed rate constants for successive catalytic cycles given in Table VI.

The data presented in Table VI also indicate that the cobalt(II)-phthalocyanine complex is participating in a closed catalytic sequence of reaction steps in which the active catalytic center is regenerated in situ. There appears to be a minor loss of catalytic activity on successive addition and oxidation of S(IV). The reduction in the catalytic efficiency of Co(II)-TSP may be attributed to irreversi-

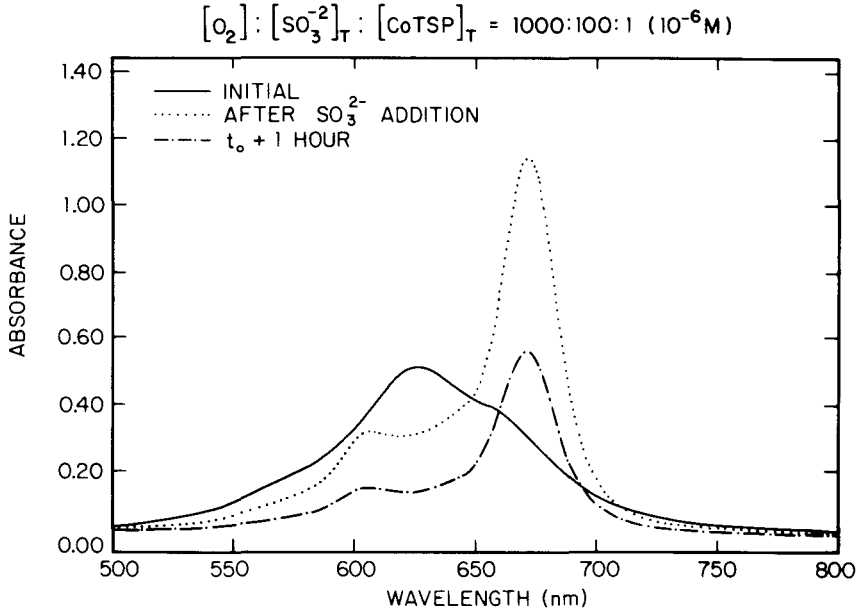

Figure 8. Visible absorption spectra for Co(II)-TSP before, during and after addition of sulfite at pH 6.7. Growth of the absorption maximum at 670 nm occurs after sulfite addition. Before addition, λ_{max} = 636 nm.

ble decomposition of the macrocylic ligand structure, which is susceptible to oxidative degradation [71].

Since metal-phthalocyanine complexes are common dye molecules and potential sensitizers for the photolytic activation of dioxygen, catalysis of autoxidation reactions by Co(II)-TSP may be light-dependent. To test this hypothesis, experi-

Table VI. Tests of Catalytic Activity with Successive Additions of Sulfite at pH 6.7[a]

Catalytic Cycle	k_{obs} (10^4 s^{-1})
1	7.46
2	7.43
3	6.85
4	6.35
5	5.60

[a] $[Co(II)\text{-}TSP]_o = 10^{-6}$ *M*; $[SO_3^{2-}]_o = 10^{-4}$ *M*; $[O_2]_o = 10^{-3}$ *M*; μ = 0.4 with 10^{-6} *M* EDTA.

ments were conducted in the presence and absence of conventional fluorescent room light. The kinetic results described in the previous sections of this paper were derived from reactions carried out under background illumination. In the absence of an external light source, autoxidation of sulfite proceeded very slowly after rapid formation of an intermediate Co(II)-TSP/SO_3^{2-}/O_2 complex. The solid and dashed lines in Figure 9, A_{213} and A_{670}, correspond to the absorbance due to sulfite and the intermediate species, respectively. The decline in the concentration of S(IV) and the cobalt-sulfite-dioxygen adduct was accelerated dramatically on exposure of the reactant solution to room light. Reactions catalyzed by Fe(II)-TSP and Mn(II)-TSP seemed to be insensitive to the effects of irradiation. The origin of this apparent "photoassisted" catalysis is being investigated in greater detail.

Variation of the central metal atom in the structure of the phthalocyanine complex produced noticeable changes in the rate of oxidation of sulfite as shown in Table VII. Co(II)-TSP exerted the most pronounced catalytic effect on the

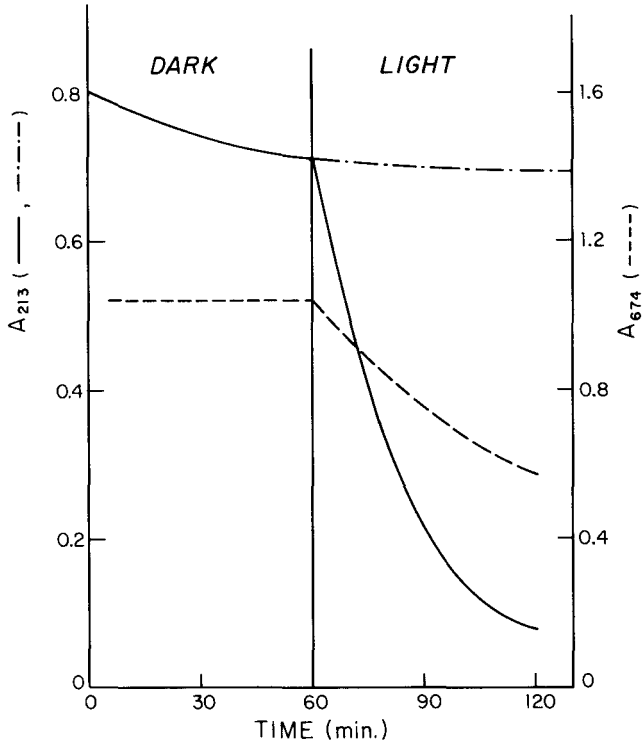

Figure 9. Relative effect of fluorescent room light on the catalytic autoxidation of sulfite. The solid line refers to absorbance of SO_3^{2-} and the dashed line refers to the absorbance of all monomeric Co(II) complexes.

Table VII. Effect of a Variation in the Central Metal on Rate of Autoxidation of S(IV) at pH 9.2[a]

Metal	k_{obs} (10^4 s^{-1})
Co(II)	18.30
Fe(II)	2.23
Mn(II)	0.24
Cu(II)	$\simeq 0$
Ni(II)	$\simeq 0$
V(IV)	$\simeq 0$

[a] $[S(IV)]_o = 10^{-4}$ *M*; $[O_2]_o = 10^{-3}$ *M*; $\mu = 0.4$ *M*.

autoxidation process. Similar trends in catalytic activity have been reported by Hoffman and Lim [51] for the reaction of hydrogen sulfide with molecular oxygen in aqueous solution and by Kropf [74] and Kropf and Hoffman [75] for the liquid-phase autoxidation of hydrocarbons.

Presumably, the differences in the catalytic properties of the various metal-phthalocyanines can be explained in terms of the relative capacities of the complexes to bind molecular oxygen. Many square planar Co(II) complexes undergo solution-phase reactions with Lewis bases to yield five-coordinate derivatives of the type Co(II)(L)(B):

$$\text{Co(II) L} + \text{B} \rightleftharpoons \text{Co(II)(L)(B)} \tag{28}$$

$$\text{Co(II)(L)(B)} + \text{O}_2 \rightleftharpoons \text{Co(II)(L)(B)} - \text{O}_2 \tag{29}$$

where L = tetradentate phthalocyanine, porphyrin or Schiff-base ligand
B = electron-donor attached to an axial coordination site

Coordination of an axial base promotes the reversible formation of mononuclear dioxygen adducts (Equation 29) in which the bonding of O_2 to the metal center is represented nominally either as a superoxide ion (O_2^-) coordinated to Co(III) or as a singlet oxygen bound to Co(II) [76,77]. Electron spin resoncance spectroscopic measurements and theoretical calculations suggest that the structure of metal-dioxygen is correctly assigned as cobalt(III)-superoxide [77]. A qualitative molecular orbital (MO) description predicts that bonding of oxygen to cobalt(II) occurs in a bent end-on configuration involving overlap of the singly occuped d_{π}^2 orbital on Co(II) with an antibonding π-orbital (π^*) of O_2 as depicted in Figure 10. According to this simplified model, there is only a minor cobalt d_{π}-oxygen p_{π}

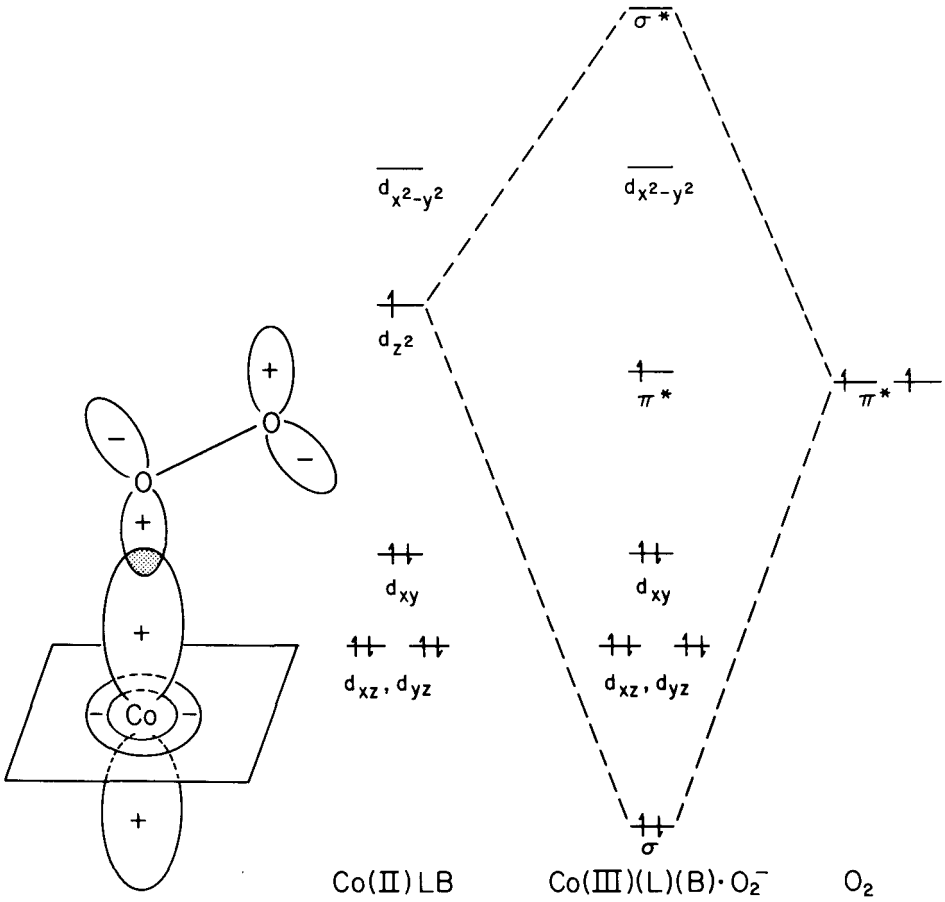

Figure 10. Qualitative molecular orbital description of the bonding between Co(II)(L)(B) complex and dioxygen. Sigma bond formation results from overlap of electron density between the singly occupied d_{z2} orbital on Co and the π^* MO of O_2. L denotes a planar tetradentate ligand, and B denotes an axial base.

interaction and the unpaired electron resides primarily in the remaining π^* MO on O_2.

Studies of the catalytic properties of cobalt-substituted model hemesystems have demonstrated that the stability and reversibility of formation of metal-dioxygen adducts are affected by the nature of the ligand B coordinated in the axial position trans to O_2 [77]. For example, thermodynamic data for this reaction suggest that the oxygen affinity of metal complexes is associated with the σ-donor, π-donor and π-acceptor electronic properties of B [78]. These correlations follow the general notion that increased electron density at the metal atom due to axial coordination

of B enhances the bonding interaction with oxygen, thereby promoting an "intramolecular redox reaction" of Co(II)-O_2 to give CO(III)-O_2^-. Complexes of Fe(II) and, to a much lesser extent, Mn(II) may bind dioxygen in a similar fashion. The electron configurations of VO^{2+}, Cu(II) and Ni(II) do not favor coordination of axial ligands. Consequently, synthetic dioxygen adducts of V(IV), Ni(II) and Cu(II) complexes are virtually unknown [79].

In aqueous solution, Fe(II)- and Co(II)-TSP undergo reversible oxygenation to form dimeric oxygen adducts in which the product is formulated as the μ-peroxo species M(III)-O_2^{2-}-M(III) [52]. Oxygenation of Fe(II)-TSP proceeds spontaneously at neutral pH (6.5) via the following sequence of reactions:

$$\text{Fe-(TSP)}(H_2O)_2^{4-} + O_2 \underset{K_1}{\rightleftharpoons} \text{Fe-(TSP)}(H_2O)O_2^{4-} + H_2O \quad (30)$$

$$\text{Fe-(TSP)}(H_2O)O_2^{4-} + \text{Fe-(TSP)}(H_2O)_2 \underset{K_2}{\rightleftharpoons} [\text{Fe-(TSP)}(H_2O)]_2O_2 + H_2O \quad (31)$$

The values of the equilibrium constants K_1 and K_2 are 2×10^4 and 4×10^7 M^{-1}, respectively [80,81]. Formation of the corresponding 2:1 cobalt complex occurs only under strongly alkaline conditions (pH $\geq$ 12). Analysis of the kinetic data supported the assertion mechanism involves two discrete stages:

$$\text{Co-(TSP)}(H_2O)(OH)^{5-} + O_2 \rightleftharpoons \text{Co-(TSP)}(OH)O_2^{5-} + H_2O \quad (32)$$

$$\text{Co-(TSP)}(H_2O)(OH)^{5-} + \text{Co-(TSP)}(OH)O_2^{5-} \rightleftharpoons [\text{Co-(TSP)}(OH)]_2O_2^{10-} + H_2O \quad (33)$$

in which the initial oxygenation step constitutes the rate-limiting process with a second-order rate constant of 3.24 M^{-1}-s^{-1} at pH 13 [82].

The relative efficiencies of Co(II)- and Fe(II)-TSP as catalysts for the autoxidation of SO_3^{2-} seem to be related to the stability of the monomeric dioxygen adducts in aqueous solution. Hoffmann and Lim [51] proposed that a 1:1 Co(II)-TSP-O_2 addition product was the active catalytic center in the oxidation of HS^-. Mass et al. [48] also concluded that in polymer-supported Co(II)-TSP systems the reactive species for the autoxidation of thiols was a monomeric adduct. Increased catalytic activity in the heterogeneous phthalocyanine system relative to the homogeneous Co(II)-TSP complex may reflect constraints imposed on the dimerization reaction by the surface structure of the solid support. Spectral changes observed during the current study of the autoxidation of sulfite are consistent with the hypothesis that coordination of SO_3^{2-} in an axial position of Co(II)-TSP is a necessary prelude to the formation of a six-coordinate 1:1 cobalt-dioxygen adduct at pH 6.7 and 9.2. Complexation of sulfite and O_2 by Co(II)-TSP leads ultimately to a more rapid autoxidation step. Production of a peroxo-dimer Co(III)-TSP-O_2^{2-}Co(III) would occur only at high concentrations of hydroxide.

Mechanistic Interpretation of Kinetic Observations

Based on the experimental observations and kinetic data obtained to date, two alternative mechanisms can be proposed to describe the detailed molecular processes involved in the catalytic autoxidation of sulfite. They include a two-electron transfer, bisubstrate complexation pathway, and a one-electron transfer, chain reaction sequence. Each of these mechanistic possibilities will be presented and examined for consistency with experimental measurements.

Two-Electron Transfer, Bisubstrate Complexation Pathway

The catalytic activity of metal-phthalocyanines in aqueous solution was documented initially by Cook [83–85] for the decomposition of H_2O_2 and the oxidation of HI and later by Wagnerova and co-workers for the autoxidation of hydrazine [49], hydroxylamine [50] and cysteine [86]. As mentioned in the introduction to this chapter, these investigators compared the catalytic behavior of cobalt-, iron- and manganese-phthalocyanine complexes to the features of oxidase enzymes and peroxidase. A well known characteristic of the kinetics of enzymatic reactions is the variability of reaction orders for catalyst and substrate. Under certain conditions, the reaction order in substrate can vary between zero and one; but most likely a nonintegral value will be observed [87].

To interpret the observed kinetic behavior for the autoxidation of sulfite in terms of an enzymatic framework, a bisubstrate model for the catalytic activity of homogeneous metal-phthalocyanine complexes was developed. A rate law for this scheme was derived using the method of King and Altman [88], which is based on a standard determinant procedure used for solving a system of inhomogeneous linear equations obtained through steady-state considerations. The mechanism postulated to account for the observed kinetic behavior is the ordered-ternary complex pathway depicted symbolically in Figure 11 and given below.

$$(\text{Co(II)-TSP})_2^{4-} \underset{}{\overset{K_d}{\rightleftharpoons}} 2\ \text{Co(II)-TSP}^{2-} \tag{34}$$

$$\text{Co(II)-TSP}^{2-} + SO_3^{2-} \underset{k_{-o}}{\overset{k_o}{\rightleftharpoons}} SO_3\text{Co(II)-TSP}^{4-} \tag{35}$$

$$SO_3\text{Co(II)-TSP}^{4-} + O_2 \underset{k_{-1}}{\overset{k_1}{\rightleftharpoons}} SO_3\text{Co(III)-TSPO}_2\cdot^{4-} \tag{36}$$

$$SO_3^{2-} + SO_3\text{Co(III)-TSPO}_2^{4-} \underset{k_{-2}}{\overset{k_2}{\rightleftharpoons}} SO_3\text{Co(III)-TSPO}_2\cdot SO_3^{6-} \tag{37}$$

$$H_2O + SO_3\text{Co(III)-TSPO}_2\cdot SO_3^{6-} \underset{h\nu}{\overset{k_3}{\rightleftharpoons}} SO_3\text{Co(II)-TSPO}_2^{6-} + H_2SO_4 \tag{38}$$

ORDERED TERNARY-COMPLEX MECHANISM

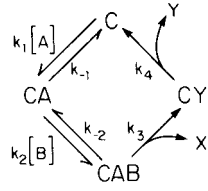

$$v = \frac{\{k_3k_4/(k_3+k_4)\}[C]_o[A][B]}{\frac{k_4(k_{-1}k_{-2}+k_{-1}k_3)}{k_1k_2(k_3+k_4)} + \frac{k_4(k_{-2}+k_3)}{k_2(k_3+k_4)}[A] + \frac{k_3k_4}{k_1(k_3+k_4)}[B] + [A][B]}$$

$C \equiv {}^{2-}(SO_3)Co(II)TSP$

$A \equiv O_2$

$B \equiv SO_3^{=}$

$X \equiv HSO_4^-$

$Y \equiv H_2O_2$

Figure 11. Theoretical rate expression obtained from the steady-state solution to the closed catalytic sequence above using the vector method of King and Altman [88].

$$SO_3Co(II)\text{-}TSPO_2^{6-} + 2H^+ \xrightarrow{k_4} SO_3Co(II)\text{-}TSP^{4-} + H_2O_2 \qquad (39)$$

$$H_2O_2 + SO_3^{2-} \xrightarrow{k_5} SO_4^{2-} + H_2O \qquad (40)$$

Equation 34 represents the formation of the reactive monomeric catalyst center (designated by C in Figure 11) from the predominant dimeric form of cobalt(II)-phthalocyanine in aqueous solution. This sequence of events is consistent with the spectral changes shown in Figure 8 that indicate a shift in the monomer-dimer equilibrium on addition of sulfite to the catalyst solution. Complexation of SO_3^{2-} by Co(II)-TSP in an axial position enhances coordination of molecular oxygen as written in Equation 36. The resulting intermediate is considered to be a mixed ligand Co(III) complex with a superoxide ion and sulfite bound at sites trans to one another about the metal center. In the proposed mechanism, this dioxygen adduct then reacts with an additional substrate ion to produce the ternary complex given in Equation 37. An intramolecular rate-limiting two-electron transfer followed by hydrolysis yields H_2SO_4 and a sulfito-cobalt(III)-peroxide derivative. After protonation, the coordinated O_2^{2-} is released as H_2O_2. Subsequently, hydrogen peroxide may be consumed via reaction with an additional molecule of substrate.

Evidence of a direct two-electron transfer redox step was reported recently by Schutten and Beelen [89], who observed the accumulation of H_2O_2 as an intermediate reduction product during the Co(II)-TSP–catalyzed autoxidation of 2-mercaptoethanol in water. Davies et al. [29] employed ^{18}O-tracer experiments to determine the source of the oxygen atoms in sulfate produced from the reaction of sulfite with O_2. The authors found that approximately one-half of the oxygen transferred to SO_3^{2-} originated from a dimeric superoxo- complex, $(NH_3)_5Co(III)\text{-}O_2^-\text{-}Co(III)(NH_3)_5$. Holt et al. [90] have shown that the ^{18}O content of the product sulfate in metal-catalyzed reaction systems varies as a linear function of the ^{18}O content of water and that at least three of the four O atoms in SO_4^{2-} are isotopically controlled by the solvent (the remaining oxygen atom originating from O_2). Finally, Yatsimirskii et al. [91] have obtained strong evidence that complexation of sulfite by a [Co(II)-l-histidine$_2$]$_2O_2$ adduct occurs before electron transfer from S(IV) to O_2. In total, these results are compatible with the reaction mechanism outlined in Equations 34–40.

The observed photocatalytic effect (Figure 9) suggests that absorption of light by a reactive intermediate such as $SO_3Co(III)\text{-}TSPO_2\cdot SO_3^{6-}$ may play a key role in the mechanism for the oxidation of sulfite. Beelen et al. [92] attributed the influence of visible light in the 600 to 700-nm wavelength range on the phthalocyanine-catalyzed autoxidation of mercaptoethanol to a shift in the equilibrium composition of the Co(II)-TSP solution in favor of the catalytically active monomeric species. An alternative explanation that is consistent with the experimental data recorded in the current study is that the reactive ternary complex may absorb radiation to generate a bound singlet oxygen species of the form $SO_3Co(II)\text{-}TSP\cdot {}^1O_2\cdot SO_3^{6-}$. This intermediate would possess more favorable spin symmetry for facile electron transfer. Cox et al. [93] have shown that metalloporphyrins give rise to singlet-excited state O_2 on irradiation at appropriate wavelengths.

In the proposed reaction mechanism, the active catalytic center is the complex $SO_3Co(II)TSP^{4-}$. The catalytic reaction cycle begins and ends with this complex. Steps leading to formation of the active center are assumed to be in rapid equilibrium and may be ignored in the initial derivation of a rate expression. In the catalytic cycle, there are three intermediates, $SO_3Co(III)\text{-}TSPO_2\cdot{}^{4-}$, $SO_3Co(III)\text{-}TSPO_2\cdot SO_3^{6-}$ and $SO_3Co(III)\text{-}TSP\cdot O_2^{6-}$, and three steady-state equations for each species. Using the method of King and Altman [88], the concentration of reactive intermediate forms of the catalyst can be expressed as:

$$[SO_3Co(II)\text{-}TSP^{4-}] \propto k_{-1}k_{-2}K_{-4} + k_{-1}k_3k_4 + k_2k_3k_4[SO_3^{2-}] \tag{41}$$

$$[SO_3Co(III)\text{-}TSPO_2\cdot{}^{4-}] \propto k_1k_{-2}k_4[O_2] + k_1k_3k_4[O_2] \tag{42}$$

$$[SO_3Co(III)\text{-}TSPO_2\cdot SO_3^{6-}] \propto k_1k_2k_4[O_2][SO_3^{2-}] \tag{43}$$

$$[SO_3Co(II)\text{-}TSPO_2^{6-}] \propto k_1k_2k_3[O_2][SO_3^{2-}] \tag{44}$$

The mass balance for the total catalyst concentration is given by:

$$[SO_3Co(II)\text{-}TSP^{4-}]_T = [SO_3Co(II)\text{-}TSP^{4-}] + [SO_3Co(III)\text{-}TSPO_2\cdot^{4-}] + [SO_3Co(III)\text{-}TSPO_2\cdot SO_3^{6-}] + [SO_3Co(III)\text{-}TSPO_2^{6-}] \quad (45)$$

Since the rate of overall reaction is defined by the rate of the slow step in the closed cycle, the rate can be written as:

$$\nu = \frac{-d[SO_4^{2-}]}{dt} = k_3[SO_3Co(III)\text{-}TSPO_2\cdot SO_3^{6-}] \quad (46)$$

where, from steady-state considerations and from Equation 44:

$$[SO_3Co(III)TSP\text{-}O_2\cdot SO_3^{6-}] = \frac{k_1k_2k_4[SO_3Co(II)\text{-}TSP^{4-}]_T[O_2][SO_3^{2-}]}{D} \quad (47)$$

for which

$$D' = k_4(k_{-1}k_{-2} + k_{-1}k_3 + k_2k_3[SO_3^{2-}]) + k_1k_4(k_{-2} + k_3)[0_2] + k_1k_2(k_3 + k_4)[O_2][SO_3^{2-}] \quad (48)$$

Substitution of Equation 47 into Equation 46 gives the following theoretical rate expression for the formation of sulfate (Figure 12):

$$\nu = \frac{\{k_3k_4\ /(k_3 + k_4)\}[SO_3Co(II)\text{-}TSP^{4-}]_T[SO_3^{2-}][O_2]}{D'} \quad (49)$$

where

$$D' = \frac{k_4(k_{-1}k_2 + k_{-1}k_3)}{k_1k_2(k_3 + k_4)} + \frac{k_4(k_{-2} + k_3)}{k_2(k_3 + k_4)}[O_2] + \frac{k_3k_4}{k_1(k_3 + k_4)}[SO_3^{2-}] + [O_2][SO_3^{2-}] \quad (50)$$

Equation 48 can be reduced to the form:

$$\nu = \frac{k'[SO_3Co(II)\text{-}TSP^{4-}]_T[SO_3^{2-}][O_2]}{K_A + K_B[O_2] + K_C[SO_3^{2-}] + [O_2][SO_3^{2-}]} \quad (51)$$

The constants K_A, K_B and K_C each represent the coefficients of the terms in the denominator of the rate expression as defined by Equation 50. The kinetic expression given by Equation 51 must be modified to account for the rapid equilibria that precede the catalytic cycle involving $SO_3Co(II)\text{-}TSP^{4-}$ as the active center. Concentration of the active species can be expressed in terms of the dimer dissociation constant K_d and the formation constant for the initial sulfito complex:

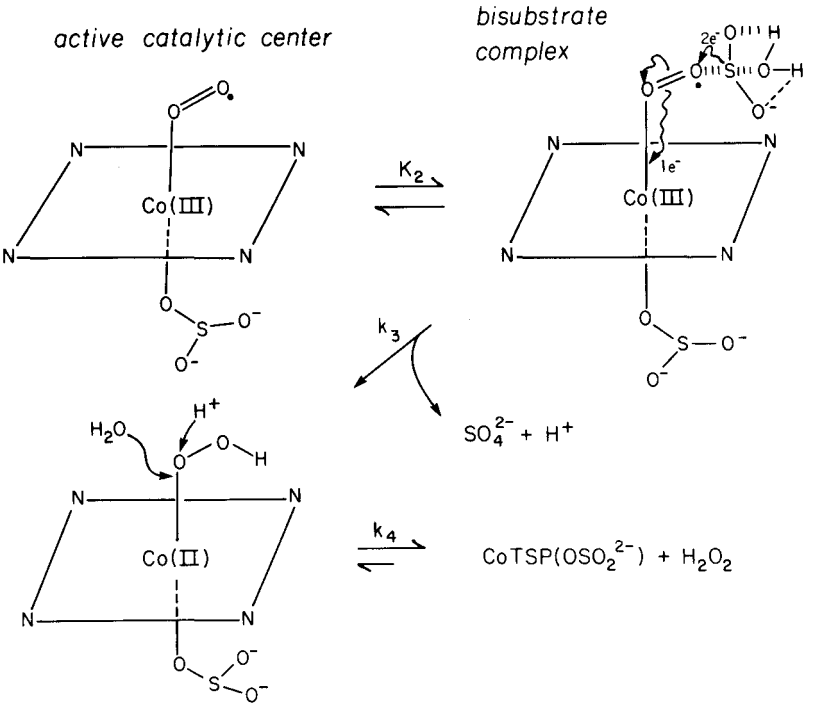

Figure 12. Schematic representation of the proposed catalytic reaction mechanism starting with the Co(II)-TSP sulfito complex as the active catalytic center. Reaction proceeds via the formation of a ternary dioxygen adduct and results in the formation of hydrogen peroxide as an intermediate reduction production of oxygen.

$$K_d = [\text{Co(II)-TSP}]^2/[(\text{Co(II)-TSP})_2^{4-}]^2 \quad (52)$$

$$\beta = [\text{SO}_3\text{Co(II)-TSP}^{4-}]/[\text{Co(II)-TSP}][\text{SO}_3^{2-}] \quad (53)$$

Equations 52 and 53 can be combined to yield:

$$[\text{SO}_3\text{Co(II)-TSP}^{4-}] = \beta K_d^{1/2}[(\text{Co(II)-TSP})_2^{4-}]^{1/2}[\text{SO}_3^{2-}] \quad (54)$$

Further simplification of Equation 54 is possible because $[SO_3^{2-}]_o >> [(Co(II)\text{-}TSP)_2]_o$. This condition allows the approximation that the concentration of sulfite in solution is relatively constant with respect to the amount coordinated in the active complex, $SO_3Co(II)\text{-}TSP^{4-}$, such that:

$$[\text{SO}_3\text{Co(II)-TSP}^{4-}]_T \simeq K'[(\text{Co(II)-TSP})_2^{4-}]^{1/2} \quad (55)$$

where $K' = \beta K_d^{1/2}[SO_3^{2-}]$ (i.e., K' is a pseudo-equilibrium constant). Substitution of Equation 55 into Equation 51 gives an approximate overall rate expression:

$$\nu = \frac{k'K'[(Co(II)\text{-}TSP)_4^{2-}]^{1/2}[SO_3^{2-}][O_2]}{K_A + K_B + K_C\,[SO_3^{2-}] + [O_2][SO_3^{2-}]} \tag{56}$$

The final rate law (Equation 56) can be simplified for the experimental pseudo-order reaction conditions, $[O_2] >> [SO_3^{2-}]$ such that $K_B[O_2] >> K_A$, $K_C[SO_3^{2-}]$ to obtain:

$$\nu = \frac{k'K'[(Co(II)\text{-}TSP)_2^{4-}]^{1/2}[SO_3^{2-}]}{K_B + [SO_3^{2-}]} \tag{57}$$

Two extremes can be considered for the reduced form of the theoretical rate law. If $K_B >> [SO_3^{2-}]$, Equation 57 becomes

$$\nu \simeq k'_\beta K_d^{1/2}[(Co(II)\text{-}TSP)_2^{4-}]^{1/2}[SO_3^{2-}]^2 \tag{58}$$

Similarly, when $[SO_3^{2-}] >> K_B$

$$\nu \simeq k'_\beta K_d^{1/2}[(Co(II)\text{-}TSP)_2^{4-}]^{1/2}[SO_3^{2-}] \tag{59}$$

The kinetic expressions for these limiting cases can be compared with the experimentally observed rate laws measured at pH 6.7

$$\nu_{obs} = k_{obs}[Co(II)\text{-}TSP]^{0.3}[SO_3^{2-}] \tag{60}$$

and pH 9.2

$$\nu_{obs} = k_{obs}[Co(II)\text{-}TSP][SO_3^{2-}] \tag{61}$$

In neutral solution, a fractional-order dependence of 0.3 in catalyst concentration is observed, whereas Equation 58 predicts a one-half order dependence on the dimeric form of Co(II)-TSP. Nonintegral reaction orders arise frequently in polar reactions when the principal reactive species is derived from the dissociation of a dimer [94]. Reevaluation of k_{obs} as a function of [Co(II)-TSP] in the presence of EDTA yielded a reaction order of approximately 0.5. Schelly et al. [72] also reported that divalent metal phthalocyanines tend to form higher-order oligomers in aqueous solution at high ionic strength. Consideration of the equilibria between higher-order aggregate species in the development of a theoretical rate expression would further reduce the apparent order in Co(II)-TSP. Since dimeric and polymeric phthalocyanine species are the dominant forms of the complex in solution at pH 6.7, a nonintegral dependence on total added Co(II)-TSP seems consistent with the assumption that the monomer is actually the active form of the catalyst.

At pH 9.2, a first-order dependence on the catalyst concentration is observed. This result is consistent with the kinetic formulation described in the preceding paragraphs if the dimeric form of Co(II)-TSP is no longer assumed to be the dominant species. Cookson et al. [95] presented evidence for a shift in the monomer-dimer equilibrium toward the monomer with an increase in pH. Under alkaline conditions, the remaining solvent molecules in the coordination sphere of Co(II)-TSP^{2-} are replaced by hydroxide groups (OH^-), resulting in increased stability of monomeric complexes such as (HO)Co(II)-TSP^{3-}, $(HO)_2$Co(II)-TSP^{4-} and HOCo(III)-$TSPO_2{\cdot}^{3-}$. In this situation, the prior equilibrium designated by Equation 34 could be neglected. Consequently, the theoretical rate expression would show a first-order dependence in catalyst, as indicated in Equation 61.

The postulated mechanism appears to explain the kinetic and spectral data for a broad range of reaction conditions. The extremes described by Equations 56 to 58 account for the slight shifts in the reaction order of S(IV) to values greater than unity, and the apparent zero-order dependence on $[O_2]$. A schematic representation of the two-electron transfer complexation pathway is presented in Figure 12 for the pH range in which sulfite (SO_3^{2-}) is the principal reactive S(IV) species in solution.

A variant of the proposed mechanism occurs when SO_3^{2-} reacts with SO_3Co(III)-$TSPO_2{\cdot}^{4-}$ without formation of a ternary complex of sufficiently long lifetime to be kinetically significant. This type of mechanism was originally suggested by Theorell and Chance [96]. The theoretical rate expression for this second alternative is identical in form to that given by Equation 50, except that the constant terms K_A, K_B and K_C are defined by different combinations of rate constants.

To verify the applicability of Equation 55 to the experimental measurements, a double-reciprocal analysis of the initial rate data was performed. Rearrangement of Equation 55 gives

$$1/\nu_o = (1 + K_A/[O_2][SO_3^{2-}] + K_B[SO_3^{2-}] + K_C/[O_2])/\nu_o \tag{61}$$

where $\nu_o = (k_3k_4/k_3 + k_4)\beta K_d^{1/2}[SO_3^{2-}][Co(II)TSP)_2^{4-}]^{1/2}$

$K_A = k_4(k_{-1}k_2 + k_{-1}k_3)/k_1k_2(k_3 + k_4)$

$K_B = k_4(k_{-2} + k_3)/k_2(k_3 + k_4)$

$K_C = k_3k_4/k_3 + k_4)$

A plot of $1/\nu_o$ vs $1/[SO_3^{2-}]_o$ at constant $[O_2]_o$ should be linear with a slope of:

$$(K_A/[O_2] + K_B^1)/\nu_o \tag{63}$$

and an intercept on the $1/\nu_o$ axis of:

$$(1 + K_C/[O_2])/\nu_o \tag{64}$$

Figure 13 shows the Lineweaver-Burk plots for the catalyzed autoxidation of sulfite at pH 6.7 and 9.2 [87]. The linearity of these functions lends strong support for the postulated ternary-complex mechanism.

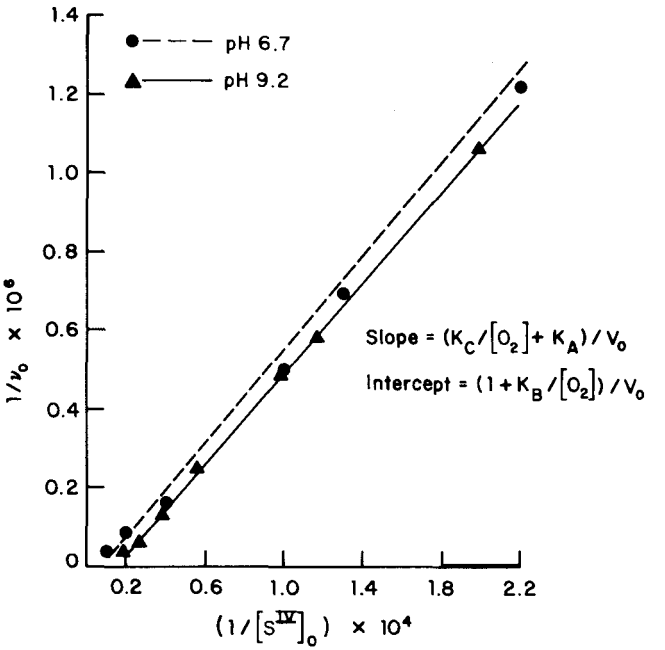

Figure 13. Lineweaver-Burk plots for the initial rate of oxygen depletion v_o, as a function of $[S(IV)]_o$ at pH 6.7 (A) and pH 9.2 (B). Reaction conditions: $[O_2]_o = 2.5 \times 10^{-4}$ *M*, [Co(II)-TSP]$_o = 1 \times 10^{-6}$ *M*, T = 25.0 C, and $\mu = 0.4$ *M*.

Analysis of the variation in reaction rate as a function of ionic strength (μ) provides evidence in support of the Theorell–Chance scheme. If $k_3 >> k_{-2}$, then the rate-limiting step is defined by Equation 36, in which two negatively charged ions (SO_3^{2-} and $SO_3Co(III)\text{-}TSPO_2{\cdot}^{4-}$) react to form an intermediate species bearing an overall net negative charge. The "primary salt effect" states that ionic reactions between ions of the same charge (i.e., both reactants are either positively or negatively charged) will proceed at a faster rate upon an increase in the ionic strength of the medium. From the Debye–Hückel theory, it can be shown that:

$$\log k = \log k_o + 1.02\, Z_a Z_b \mu^{1/2} \tag{65}$$

in which $Z_a(SO_3^{2-}) = -2$ and $Z_b(SO_3Co(III)\text{-}TSPO_2{\cdot}^{4-}) = -4$. Even though the experimental conditions ($\mu > 0.1$) exceed the upper boundary for strict applicability of the Debye–Hückel theory ($\mu < 0.01$), a positive slope for a plot of $-\log k_{obs}$ vs $\mu^{1/2}$ (m = 1.47, $R^2 = 0.9973$) was obtained at pH 9.2. In general, the reaction rate increases with increasing ionic strength.

One-Electron Transfer Chain Reaction

An alternative mechanism for the catalytic action of Co(II)TSP on the autoxidation of sulfur dioxide is outlined in Figure 14. In this sequence of steps, the ternary

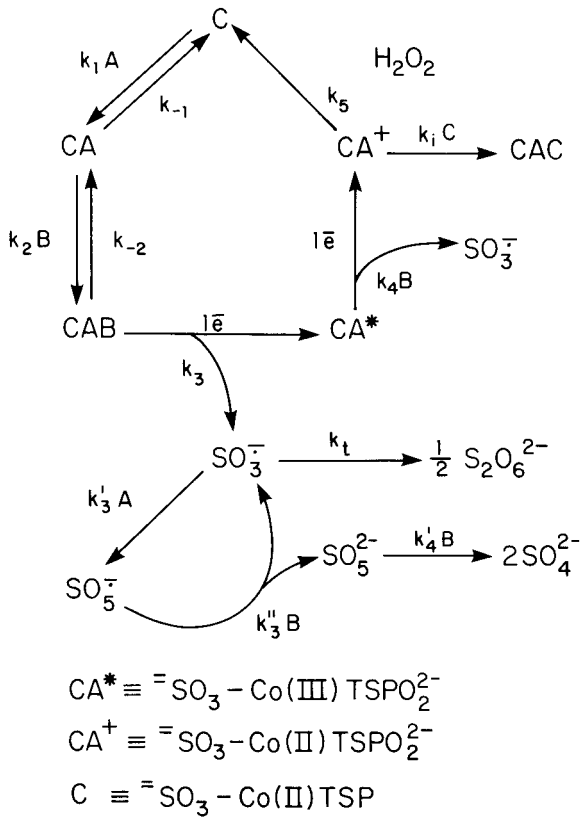

Figure 14. Alternative reaction mechanism for the Co(II)-TSP–catalyzed autoxidation of sulfite involving a one-electron transfer radical pathway in which the complex $SO_3Co(III)$-$TSPO_2^{\cdot 4-}$ acts as the primary chain-reaction initiator.

dioxygen-sulfito complex initiates the catalytic cycle via a chain reaction process identical to that described by Backström [37] and several other investigators. An additional one-electron transfer to the reduced form of the ternary complex would yield H_2O_2 as an intermediate reduction product. If the complexation equilibria are attained rapidly relative to initiation of the free-radical chain process, then the theoretical kinetic expression would be of the form:

$$\nu = k'[M^{n+}]^{0.5}[SO_3^{2-}]^{1.5} \tag{66}$$

where $[M^{n+}] = [SO_3Co(III)\text{-}TSPO_2^{\cdot 4-}]$ and $[SO_3Co(III)\text{-}TSPO_2^{\cdot 4-}] \simeq \beta K_d^{1/2}[Co(II)\text{-}TSP)_2^{4-}]^{1/2}[SO_3^{2-}][O_2]$. Substitution of these relationships into Equation 66 gives a rate law that is second-order in sulfite and first-order in oxygen. These concentration dependencies are not observed under the experimental conditions employed in the current study; therefore, the one-electron transfer mechanism is an unlikely candidate.

Alternative one-electron transfer or two-electron pathways involving the μ-superoxo complex of Co(II)-TSP can be considered as suggested by Davies

et al. [29] for $(NH_3)_5Co(III)O_2Co(II)(NH_3)_5^{5+}$ and by Yatsimirskii et al. [91] for (L-histidine)$_2$ Co(III)O_2Co(II)(L-histidine)$_2$. In this mechanism, the μ-superoxo complex, $(CoTSP)_2O_2^{4-}$, is the active catalytic center and it reacts as follows:

$$(\text{Co-TSP})_2O_2^{4-} + SO_3^{2-} \xrightarrow{\text{slow}} SO_4^{2-} + \text{Co(II)-TSP} + \text{Co(IV)-TSPO} \quad (67)$$

$$\text{Co(IV)-TSPO} + SO_3^{2-} \longrightarrow SO_4^{2-} + \text{Co(II)-TSP} \quad (68)$$

or

$$(\text{Co-TSP})_2O_2^{4-} + SO_3^{2-} \xrightarrow{\text{slow}} \text{Co(III)-TSPO}_2\text{Co(II)-TSP}^{5-} + SO_3^{\cdot-} \quad (69)$$

$$\text{Co(III)-TSPO}_2\text{Co(II)-TSP}^{5-} + SO_3^{\cdot-} \longrightarrow \text{Co(II)-TSPO}_2^{4-} + SO_3 + \text{Co(II)-TSP}^{2-} \quad (70)$$

$$SO_3 + H_2O \longrightarrow H_2SO_4 \quad (71)$$

$$\text{Co(II)-TSPO}_2^{4-} + 2H^+ \longrightarrow \text{Co(II)-TSP}^{2-} + H_2O_2 \quad (72)$$

The alternative mechanistic pathways, summarized by Equations 67–72 seem to be less feasible chemically than the proposed bisubstrate complexation scheme. For example, the electron configuration of cobalt does not readily permit formation of the nominally Co(IV) oxide intermediate as defined by Reaction 66. These mechanisms also predict a second-order rate dependence on the concentration of the Co(II)-TSP monomer (or first-order as the dimeric complex) as well as a first-order dependence on $[O_2]$. Such conditions are clearly at odds with the experimental observations.

Research in these areas is continuing with an examination of the catalytic role of simple hexaaquo metal ions and transition-metal complexes using stopped-flow/temperature-jump relaxation techniques to determine the kinetic details of the complexation and electron transfer steps. The nature of the innersphere intermediates is being elucidated further by ESR and resonance Raman spectroscopic measurements.

Effect of Metal-Catalyzed Autoxidation on the Formation of Sulfate Aerosols

The central theme of the current research explores the contribution of condensed-phase chemical processes to the transformation of sulfur dioxide to sulfuric acid in the atmosphere. The hypothesis set forth in the introduction to this chapter postulates that metal-complexation reactions are key steps in the mechanistic pathway for the catalyzed autoxidation of SO_2 dissolved in aqueous microdroplets. Kinetic data obtained under carefully controlled experimental conditions demon-

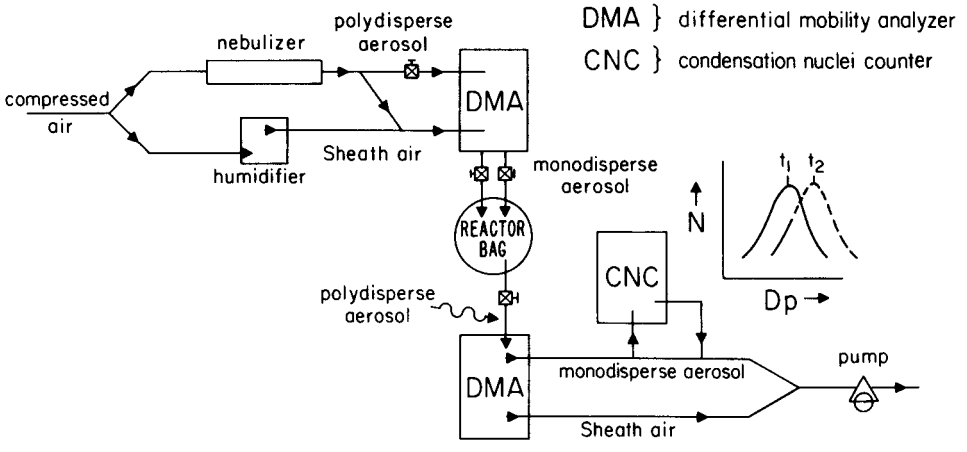

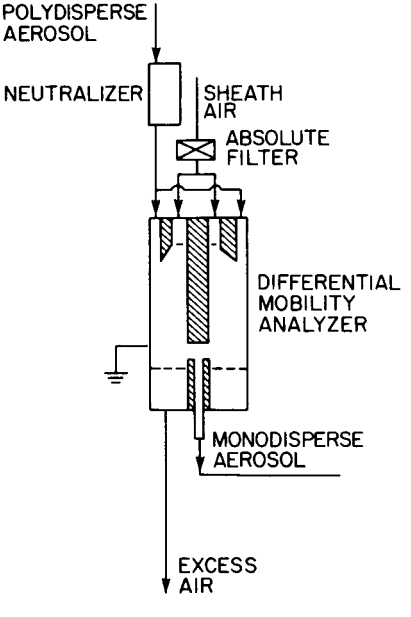

Figure 15. Schematic diagram of the experimental apparatus used to measure aerosol particle growth rates. Details of the design of the DMA are also shown.

strate that transition metal species capable of reversibly binding molecular oxygen function as effective catalysts for the oxidation of sulfite by O_2 in bulk aqueous solution. To evaluate the efficiency of the pathway under droplet-phase conditions, a series of experiments was conducted to measure the influence of the model phthalocyanine catalysts on the growth of sulfate aerosol particles.

A schematic diagram of the experimental system employed in this study is shown in Figure 15. A differential mobility analyzer (DMA) was used to initially generate an aerosol of known size and composition and then for the measurement of changes in particle diameter following the condensed-phase oxidation of SO_2. Particles are charged at the DMA inlet to achieve a Boltzmann equilibrium charge distribution on the aerosol. For the particle size range under investigation (<0.2 μm), virtually all of the particles have either 0 or ±1 unit of electrical charge. Particles are classified according to electrical mobility as the aerosol flows through the cylindrical condensor assembly of the DMA as shown in Figure 16. The voltage between the collecting rod of the condensor and the outer cylinder is varied until particles are detected by the condensation nuclei counter (CNC). At the appropriate voltage, particles have the correct electrical mobility to penetrate the slit to the

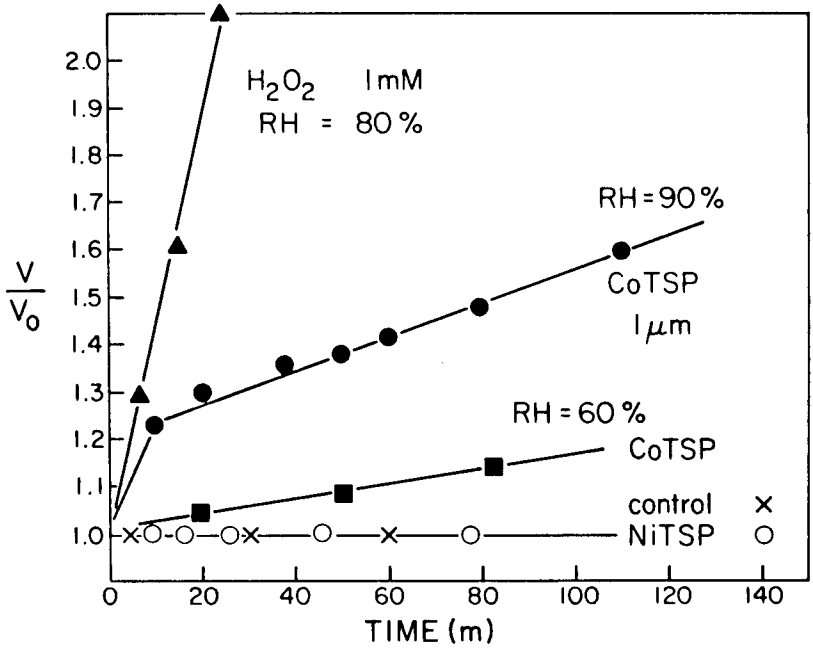

Figure 16. Preliminary experimental data showing the increase in the volume of monodisperse aerosol particles as a function of time. Particle growth rate was caused by catalytic Co(II)-TSP autoxidation of SO_2 or by reaction of SO_2 with H_2O_2. Initial particle diameters were nominally 0.06 μm in all experiments, and the SO_2 concentrations were approximately 45 ppm.

collection rod. Because the particles are singly charged there is a unique relationship between electrical mobility and size. Liu and co-workers [97,98] have used this approach to study the growth of monodisperse aerosols on humidification and for an examination of the reactions between H_2SO_4 particles and gaseous ammonia (NH_3).

In a typical experiment, a polydisperse aerosol was generated by atomizing a 10^{-4} *M* aqueous sulfuric acid solution containing the appropriate catalyst or oxidant through a nebulizer. Diversion of the flow of vapor through the DMA permitted the selection of a monodisperse droplet phase (nominally 0.06 μm in diameter) before initiation of the oxidation reaction. Sulfur dioxide was injected directly into the opaque plastic reactor bag and the growth of the aerosol particles was monitored as a function of time using a second DMA and CNC. The experiments were conducted in the dark at constant temperature and relative humidity.

Some of the SO_2 gas introduced to the reaction chamber will dissolve in the aqueous droplets according to Henry's law. Calculations by Schwartz and Freiberg [99,100] suggest that dissolution of SO_2 is instantaneous with respect to the solution-phase reaction time for droplet diameters of <1.0 μm. When a molecule of sulfur dioxide is oxidized to sulfate, another molecule plus additional water will dissolve, to maintain phase equilibrium. Addition of SO_2 and H_2O to the droplet causes an increase in the volume of the aerosol particle. The volume growth rate of the particle is directly related to the reaction rate of SO_2 oxidation within the droplet phase by:

$$\frac{dV}{dt} = \frac{1}{\rho a}(M_{SO_2} + \gamma M_{H_2O}) \frac{d}{dt} ([SO_2]_V) \tag{73}$$

where V = particle volume
ρ_a = aerosol density
M_{SO_2}, M_{H_2O} = molecular weights of SO_2 and H_2O
γ = mole ratio of H_2O to sulfate in the aerosol droplet as determined by the relative humidity
$[SO_2]$ = molar concentration of dissolved sulfur dioxide

Preliminary kinetic data obtained from the aerosol experiments are summarized in Figure 16, which shows a plot of the increase in particle size (normalized with respect to the initial monodisperse droplet volume) as a function of reaction time. Droplets containing hydrogen peroxide at an initial solution concentration of 10^{-3} *M* were observed to double in volume after approximately 20 min. The aerosol containing Co(II)-TSP also grew, but at a significantly lower rate. In a control experiment, an aerosol containing a mixture of sulfuric acid and ammonium sulfate failed to exhibit any increase in particle size on exposure to SO_2 in the absence of catalyst or oxidant. These results support the assertion that H_2O_2 acts as a highly efficient liquid-phase oxidant for nonphotolytic atmospheric conversion of aquated SO_2 to H_2SO_4.

In the model experiments with metal-phthalocyanine complexes, oxidation

of SO_2 in the presence of Co(II)-TSP at 10^{-6} *M* resulted in a 10–50% increase in particle volume over the course of 2 h. The rate of particle growth was enhanced dramatically on an increase in relative humidity from 60 to 90%, which indicates that liquid-phase reaction processes are primarily responsible for the formation of sulfate aerosol in the experimental system. In this context, it is especially interesting to note that addition of Ni(II)-TSP failed to cause an increase in particle size. The catalytic response of the rates of solution-phase reactions and aerosol growth to the presence of homogeneous transition metal complexes such as Co(II)-TSP suggests that complexation of sulfite and coordination of molecular oxygen is a feasible mechanism for the autoxidation of aquated SO_2 in atmospheric microdroplets. Further experimentation is in progress to determine the effect of light, dew point, SO_2 concentration, catalyst speciation and concentration, initial droplet pH, and solution composition on the rate of aerosol formation.

Heterogeneous Catalysis by Co(II)-TSP and Co(II)-TAP Complexes Supported on Silica Gel

Metal-catalyzed autoxidation reactions offer attractive possibilities for the development of pollution control methodologies. In commercial systems, transition metal ions are frequently associated with organic ligands as an organometallic complex, which is soluble in the solvent of interest. One major disadvantage associated with the application of homogeneous catalysis centers around the problem of separating the catalyst and products after termination of the reaction. This drawback may be overcome through attachment of the reactive complex to a solid surface. In this case a hybrid heterogeneous system is substituted for the soluble organometallic complex, thereby facilitating recovery of the catalytic species. Schutten and co-workers [101–103] have observed that the autoxidation of thio salts is accelerated in the presence of cobalt(II)-phthalocyanines bound to polyvinylamine and cross-linked styrene divinylbenzene. Catalytic autoxidation of reduced sulfur compounds in Klaus plants or sulfur dioxide in flue gas using supported metal-phthalocyanines represent two potential applications of this method.

Application of catalytic autoxidation to the formulation of an alternative technique for sulfur dioxide pollution control requires a detailed understanding of the dynamic behavior of the reaction system. The solid-supported analogs of Co(II)-TAP and Co(II)-TSP were synthesized as described in the experimental section and tested in the same batch reactor system used for the characterization of their homogeneous counterparts. The catalysts of interest are depicted schematically in Figure 17. Each of two different modes of attachment of the phthalocyanine complexes to the solid silica gel surface are illustrated in Figure 4. In one case, Co(II)-TAP is anchored to the solid support through covalent bonding of the surface ligand to the peripheral group of the macrocyclic ring, and in the second case through direct coordination of a surface imidazole functionality to the central metal atom of the phthalocyanine complex.

Kinetic data in the heterogeneous reaction systems were obtained exclusively

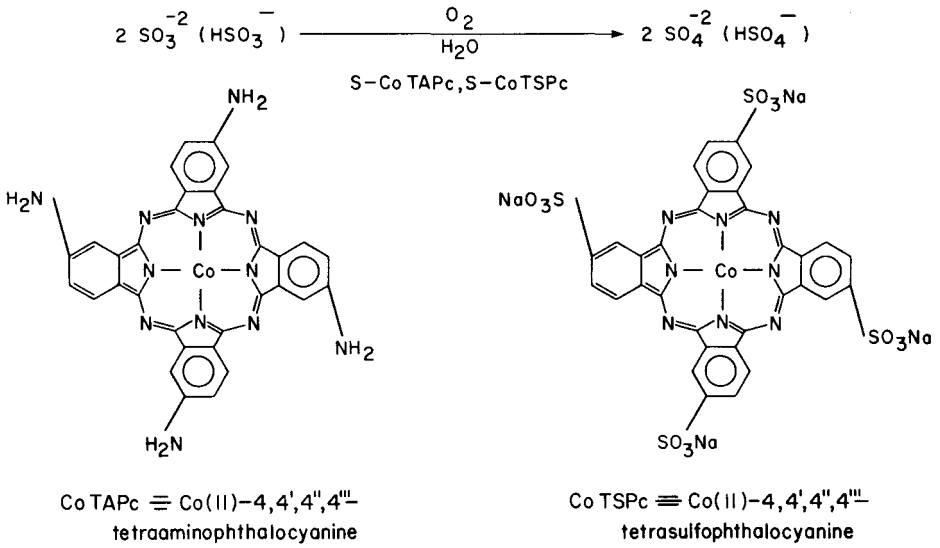

Figure 17. Stoichiometric representation of the reaction of S(IV) with oxygen in a heterogeneous suspension of cobalt phthalocyanine complexes supported on silica gel particles with a surface area of 300 m^2-g^{-1}.

by monitoring dissolved oxygen concentration with respect to time. As opposed to the concentration conditions employed in the homogeneous reactions, the heterogeneous processes were studied under pseudo-first- or zero-order concentration conditions in oxygen (i.e., $[S(IV)]_o > [O_2]_o$) such that an initial stoichiometric excess of sulfite was present in solution.

Results of the preliminary experiments in which the depletion of oxygen was measured as a function of time are summarized in Figure 18 and Table VIII. At first glance, the most effective solid-supported or "hybrid" catalyst appears to be Co(II)-TAP complex III, covalently linked to the silica gel surface through the peripheral amino group of the phthalocyanine structure. Attachment achieved via direct complexation of the surface-bound imidazole to the Co(II) center results in lower catalytic activity, and apparent deactivation of imidazole-Co(II)-TAP system IV occurs after one half-life or less of the autoxidation reaction. However, when the effect of imidazole-bonded Co(II)-TSP V is normalized with respect to the surface concentration of covalently linked Co(II)-TAP, there appear to be no differences in net catalytic activity. In this context, it should be mentioned that some of the activity exhibited by the former system under alkaline conditions may be due to dissociation of the hybrid complex from the surface to give active Co(II)-TSP in solution.

Since DMSO was used as a solvent in the preparation of Co(II)-TAP, and since McCord and Fridovich [104] have reported that DMSO is an effective catalyst for the autoxidation of sulfite, a series of control experiments was performed to

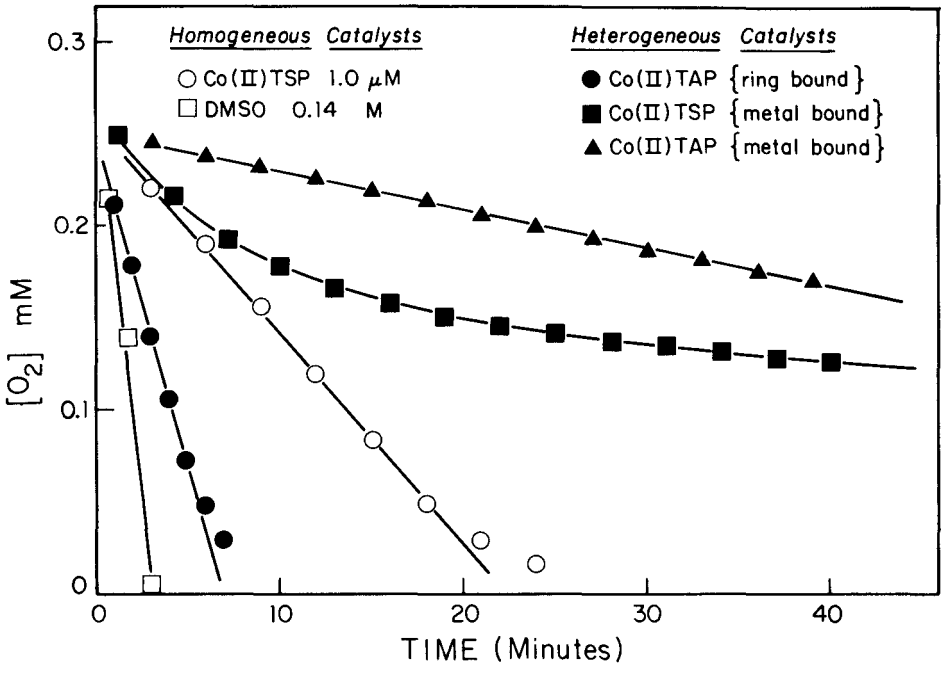

Figure 18. Comparison of the catalytic activity of various solid-supported cobalt phthalocyanine complexes toward the autoxidation of sulfite at pH 6.7 where $S(IV)_0 = 1.0$ m*M* and $O_{2_0} = 0.25$ m*M*. Additional information is provided in Table VIII.

Table VIII. Summary of Kinetics Results for Autoxidation of Sulfite at pH 6.7 in the Presence of Heterogeneous (Hybrid) Co(II)-Phthalocyanine Complexes[a]

Catalyst	$[CAT]$ (μM)	$[O_2]_0$ (mM)	$[O_2]_f$ (mM)	t_∞ (min)	τ (min)
Co(II)-TSP					
Soluble	1.0	0.260	0.003	34	11
Imidazole Hybrid	0.82[b]	0.251	0.106	120	78
Co(II)-TAP					
Soluble	1.0	0.253	0.003	3.1	1.5
Imidazole Hybrid	0.89[b]	0.253	Inactivated		43
Covalent Hybrid	20.32[b]	0.251	0.003	13	3.3
DMSO	1.4×10^5	0.260	0.003	3.9	1.8

[a] $[O_2]_0 = 2.6 \times 10^{-4}$ *M*; $[S(IV)]_0 = 1.0 \times 10^{-3}$ *M*; $[EDTA]_0 = 1 \times 10^{-5}$ *M*; T = 25.0 C; $\mu = 0.4$ *M*.

evaluate the catalytic properties of the solvent. As shown by the data in Table VIII, the reaction half-life (τ) at $[DMSO]_o = 0.14\ M$ is comparable to the value of τ for the homogeneous system containing Co(II)-TAP at $10^{-6}\ M$. However, the concentration of DMSO necessary to attain the observed reaction rate is much greater than that required for Co(II)-TAP. As a result, it seems unlikely that residual solvent from the synthetic procedure could account for the measure catalytic effects of the tetraaminophthalovyanine complexes.

Another factor complicates the analysis of liquid phase–reaction/solid phase–catalyst systems: the potential contribution of homogeneous processes promoted by dissolution of the active species from the surface of the solid support during the reaction. For example, Cohen et al. [105] have attributed the catalytic autoxidation of S(IV) in aqueous fly ash scrubbers to the presence of dissolved iron leached from the particulate matter. Unfortunately, equilibria and solution-phase species are frequently neglected in the study of heterogeneous catalysis.

In the current study, the potential role of homogeneous catalysis was examined by exposing each of the hybrid Co(II)-TAP and Co(II)-TSP complexes to the aqueous solution before initiation of the oxidation reaction. The solid-supported phthalocyanine complexes were removed by filtration before addition of sulfite. In each case, the reaction of S(IV) with O_2 was accelerated to a significant extent. Analysis by atomic absorption spectrophotometry detected trace concentrations of cobalt in the aqueous filtrate. Under alkaline conditions, dissolved cobalt exists principally as Co^{3+}. Barron and co-workers [24,34] have demonstrated that Co(III) is an effective catalyst for autoxidation of aquated SO_2. We are conducting further experiments to quantify the contribution of homogeneous processes.

Preliminary results for the heterogeneous system show that the initial rate of oxygen depletion depends on the amount of hybrid cobalt phthalocyanine initially suspended in solution. The surface coverage of Co(II)-TSP and Co(II)-TAP was determined analytically (see experimental section) to facilitate the kinetic analysis. The initial reaction rate is directly proportional to the amount of covalently bound Co(II)-TAP added to the system, as shown in Figure 19. Application of the van't Hoff method to these data suggests that the oxidation rate of sulfite exhibits a reaction order of 0.5 in effective catalyst concentration (expressed as [Co(II)]). However, because of the high porosity and surface area ($\sim 300\ m^{-2}\text{-}g^{-1}$) of the silica gel, this apparent reaction order may be influenced by mass transfer effects such as pore diffusion. The effect of diffusion on the observed reaction kinetics remains to be determined.

In general, the rates of reactions catalyzed by hybrid catalysts tend to be slower than those catalyzed by the corresponding homogeneous form of the catalyst. However, there are reports of improved catalytic activity and longer catalyst lifetimes when homogeneous species are anchored to solid surfaces. In such a heterogeneous system, the reaction is constrained to take place on the surface of the catalyst; but in the case of catalyst molecules attached to pore-wall surfaces, substrate accessibility to the active site may limit reactivity. Therefore, homogeneous catalysis is potentially more efficient in terms of the absolute amount of catalyst necessary to promote a reaction to a given extent, because all of the catalyst molecules are

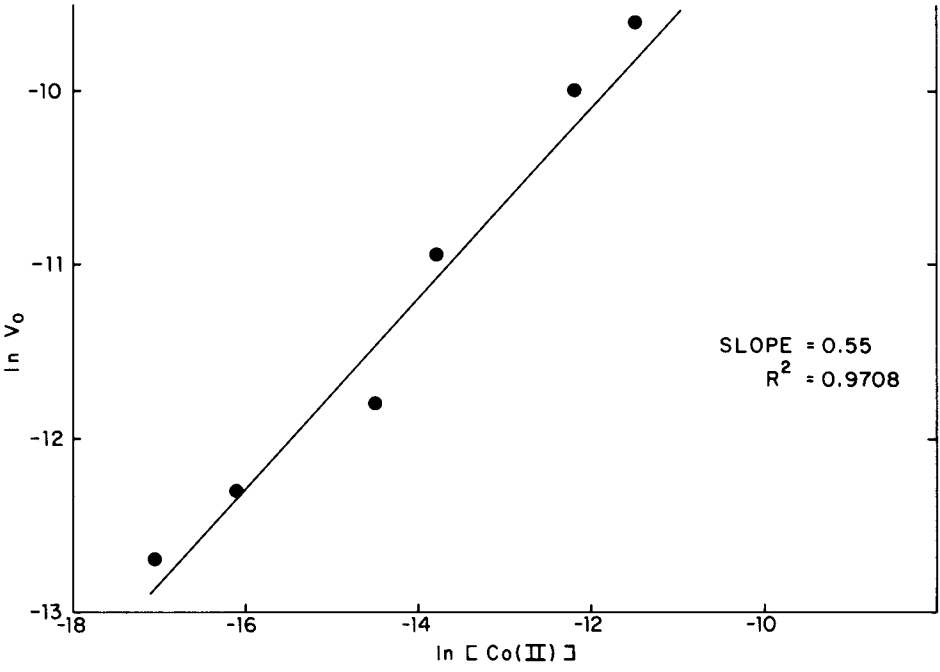

Figure 19. A van't Hoff plot of the initial oxygen depletion rate vs the initial concentration of suspended hybrid catalyst, Co(II)-TAP, attached to modified silica gel particles.

available as active centers. For a hybrid system, the catalytic properties will depend on the solid phase characteristics such as surface area, porosity and the degree of cross-linking in polymeric supports.

CONCLUDING REMARKS

As suggested previously [30,33,38], and observed in this study, certain metal-catalyzed autoxidations of sulfite proceed via the formation of discrete inner-sphere complexes between the reductant, SO_3^{2-}, and the catalyst as a prelude to electron transfer. Additional experimental evidence presented in this study, suggests that the binding and subsequent activation of dioxygen plays a significant role in the catalytic cycle. From this perspective, the most effective catalysts should involve complexes of Fe(II)/Fe(III), Mn(II)/Mn(III), Co(II)/Co(III) and V(III)/V(IV) in which the central metal is reversibly oxidized and reduced on complexation by oxygen and/or sulfite. Inhibition of catalytic activity by strong chelating and complexing agents supports this conclusion.

Certain metal-catalyzed reactions of sulfite may be enhanced by a photoassisted pathway as shown in this study for Co(II) and reported previously [39]

for Fe(III). This apparent coupling of photolytic and metal-catalyzed processes may help to explain relative differences between night- and daytime SO_2 conversion rates. More work is needed in this area to extend and apply this concept to aerosol systems.

In liquid aerosol systems, important factors to consider are the nature and roles of dissolved organic molecules that can act as competitive complexing agents for metals. For example, liquid-phase autoxidation of benzaldehyde produces benzoic acid, which can act as a suitable complexing agent (e.g., $pK_{a1} = 3.97$, $\log\beta_{11} = 1.51$ for $Cu(C_7H_6O_2)^+$) and a similar oxidation of 2-hydroxybenzaldehyde to 2-hydroxybenzoic acid produces even a stronger potential ligand (e.g., $pK_{a1} =$

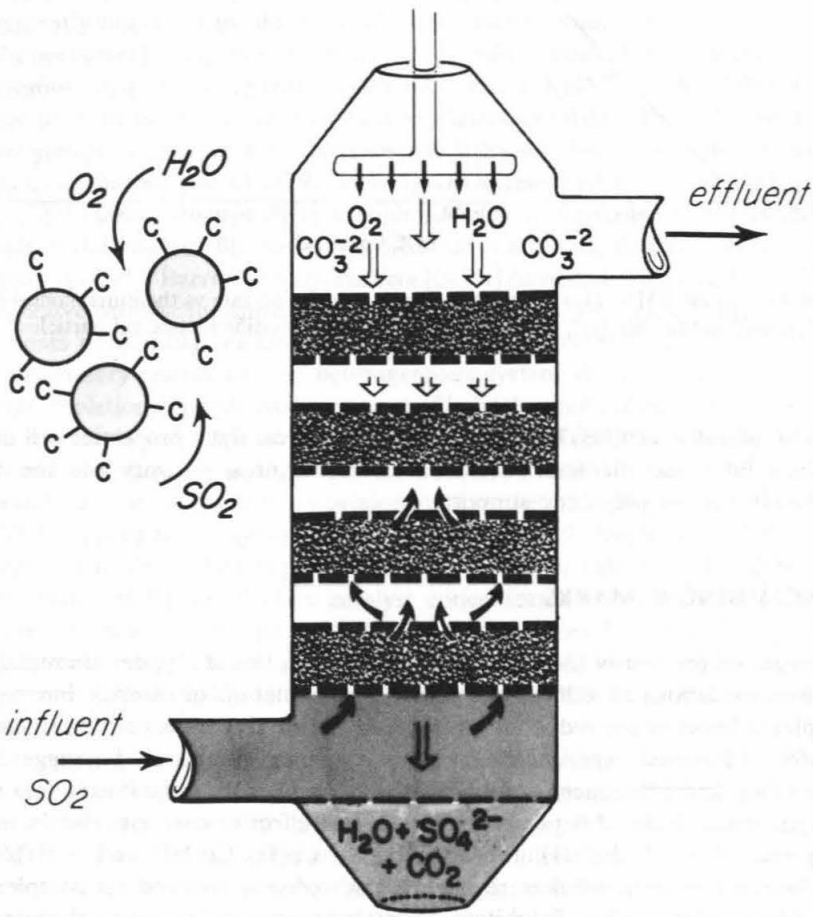

Figure 20. A potential application of polymer-supported organometallic catalysts for sulfur dioxide stack gas scrubbing is illustrated above. The active catalyst C is supported on appropriate solid supports and placed in fixed beds in a countercurrent-flow reactor.

2.78, $-\log\beta_{11} = 10.13$ for $Cu(C_7H_6O_3)^+$). The presence of complexing agents of this type will accelerate the dissolution of Fe_2O_3 and MnO_2, which are the likely sources of soluble iron and manganese in aerosol systems. As shown by Cohen et al. [105], the catalytic activity of soot-derived aerosols correlates well with the total iron released to the liquid phase.

Results of this study, along with the work of others, indicate that H_2O_2 is a major intermediate reduction product of the catalyzed oxidation of various sulfur compounds and oxidizable organic molecules. As such, metal-catalyzed autoxidation reactions in liquid aerosols may be a significant source of atmospheric peroxide [106,107]. However, accumulation of H_2O_2 would not occur to an appreciable extent in liquid aerosols that contain or are exposed to high concentrations of SO_2.

Preliminary research on hybrid organometallic catalysts has shown that attachment of homogeneous catalysts to solid surfaces results in a negligible loss of catalytic activity for the autoxidation of dissolved S(IV). Improved catalytic ability, elimination of recovery problems and longer catalyst lifetimes may be achieved with supported organometallic catalysts. Mass et al. [48] and Schutten and co-workers [89,101] have reported an enhanced catalytic autoxidation of mercaptoethanol by Co(II)-TAP attached to cross-linked polyacrylamide and polyvinylamine, respectively. Figure 20 illustrates a hypothetical countercurrent reactor with fixed beds of solid supported catalyst that could be used for SO_2 scrubbing with the production of H_2SO_4 as an alternative to limestone slurry scrubbers, which produce an unusable solid reaction product. Similarly, a fixed-bed reactor of mixed solid-supported catalysts with variable reactivity and specificity may be employed for tertiary wastewater treatment of refractory organics remaining after biological oxidation of industrial or domestic wastes. Research along these lines is being pursued presently in this laboratory.

ACKNOWLEDGMENTS

The authors acknowledge gratefully the financial support of the U.S. Environmental Protection Agency (grant R808086-01) and President's Fund/Sloan Foundation Grant administered by the California Institute of Technology. They are also indebted to their colleagues in the air pollution field, P. McMurry, G. Cass, R. Flagan, G. McRae and J. Seinfeld, for their informative discussions on the subject of aerosol chemistry. The aerosol experiments were conducted under the direction of Peter W. McMurry in the Particle Technology Laboratory, Department of Mechanical Engineering, University of Minnesota.

REFERENCES

1. Calvert, J.G., F. Su, J.W. Bottenheim and O.P. Strausz. "Mechanisms of Homogeneous Oxidation of Sulfur Dioxide in the Troposphere," *Atmos. Environ.* 12:197–226 (1978).

2. Middleton, P., C.S. Kiang and V.A. Mohnen. "Theoretical Estimates of the Relative Importance of Various Urban Sulfate Aerosol Production Mechanisms," *Atmos. Environ.* 14:463–472 (1980).
3. Möller, D. "Kinetic Model of Atmospheric Oxidation Based on Published Data," *Atmos. Environ.* 14:1067–1076 (1980).
4. Cass, G.R., and F.H. Shair. "Transport of Sulfur Oxides Within the Los Angeles Sea Breeze/Land Breeze Circulation System," in *Proceedings of the Second Joint Conference on Applications of Air Pollution Meteorology* (American Meteorological Society, 1980), pp. 320–327.
5. Cass, G.R. "Methods for Sulfate Air Quality Management with Applications to Los Angeles," PhD Thesis, California Institute of Technology, Pasadena, CA (1977).
6. Cox, R.A. "Particle Formation from Homogeneous Reactions of Sulfur Dioxide and Nitrogen Dioxide," *Tellus* 26:235–240 (1974).
7. McMurry, P.H., D.J. Rader and J.L. Smith. "Studies of Aerosol Formation in Power Plant Plumes. I. Parametrization of Conversion Rate for Dry, Moderately Polluted Ambient Conditions," *Atmos. Environ.* 15:2315–2329 (1981).
8. Smith, F.B. and G.H. Jeffrey. "Airborne Transport of Sulphur Dioxide from the U.K.," *Atmos. Environ.* 9:643–659 (1975).
9. Wilson, J.C., and P.H. McMurry. "Studies of Aerosol Formation in Power Plant Plumes. II. Secondary Aerosol Formation in the Navajo Generating Station Plume," *Atmos. Environ.* 15:2329–2339 (1981).
10. Schwartz, S.E. "Gas-Aqueous Reactions of Sulfur and Nitrogen Oxides in Liquid-Water Clouds," in *Acid Rain, Vol. 3, SO_2, NO and NO_2 Oxidation Mechanisms: Atmospheric Considerations,* J.G. Calvert, Ed. (Ann Arbor, MI: Ann Arbor Science Publishers, 1983).
11. Martin, L.R. "Kinetic Studies of Sulfite Oxidation in Aqueous Solution," in *Acid Rain, Vol. 3, SO_2, NO, and NO_2 Oxidation Mechanisms: Atmospheric Considerations,* J.G. Calvert, Ed. (Ann Arbor, MI: Ann Arbor Science Publishers, 1983).
12. Cheng, R.T., M. Corn and J.O. Frohliger. "Contributions to the Reaction Kinetics of Water-Solubles and SO_2 in Air at ppm Concentrations," *Atmos. Environ.* 5:987–1008 (1971).
13. Beilke, S., and G. Gravenhorst. "Heterogeneous SO_2-Oxidation in the Droplet Phase," *Atmos. Environ.* 12:231–239 (1978).
14. Dasgupta, P.K., P.A. Mitchell and P.W. West. "Study of Transition Metal–S(IV) Systems," *Atmos. Environ.* 13:775–782 (1979).
15. Freiberg, J. "Effects of Relative Humidity and Temperature on Iron-Catalyzed Oxidation of SO_2 in Atmospheric Aerosols," *Environ. Sci. Technol.* 8:731–734 (1974).
16. Fuzzi, S. "Study of Iron(III) Catalyzed Sulphur Dioxide Oxidation in Aqueous Solution over a Wide Range of pH," *Atmos. Environ.* 12:1439–1442 (1978).
17. Hegg, D.A., and P.V. Hobbs. "Oxidation of Sulfur Dioxide in Aqueous Systems with Particular Reference to the Atmosphere," *Atmos. Environ.* 12:241–253 (1978).
18. Kaplan, D.J., D.M. Himmelblau and C. Kanaoka. "Oxidation of Sulfur Dioxide in Aqueous Ammonium Sulfate Aerosols Containing Manganese as a Catalyst," *Atmos. Environ.* 15:763–773 (1981).
19. Larson, T.V., N.R. Horike and H. Halstead. "Oxidation of Sulfur Dioxide by Oxygen and Ozone in Aqueous Solution: A Kinetic Study with Significance to Atmospheric Processes," *Atmos. Environ.* 12:1597–1611 (1978).
20. Penkett, S.A., B.M.R. Jones and A.E.J. Eggleton. "A Study of SO_2 Oxidation in Stored Rainwater Samples," *Atmos. Environ.* 13:139–147 (1979).

21. Hayon, E., A. Treinin and J. Wilf. "Electronic Spectra, Photochemistry, and Autoxidation Mechanism of the Sulfite–Bisulfite–Pyrosulfite Systems. The SO_2^-, SO_3^-, and SO_5^- Radicals," *J. Am. Chem. Soc.* 94:47–57 (1972).
22. Sheldon, R.A., and J.K. Kochi. *Metal-Catalyzed Oxidations of Organic Compounds* (New York: Academic Press, Inc., 1981).
23. Hoffmann, M.R. "Trace Metal Catalysis in Aquatic Environments," *Environ. Sci. Technol.* 14:1061–1066 (1980).
24. Barron, C.H., and H.A. O'Hern. "Reaction Kinetics of Sodium Sulfite by the Rapid-Mixing Method," *Chem. Eng. Sci.* 21:397–404 (1966).
25. Bengtsson, S., and I. Bjerle. "Catalytic Oxidation of Sulphite in Dilute Aqueous Solutions," *Chem. Eng. Sci.* 30:1429–1435 (1975).
26. Brimblecombe, P., and D.J. Spedding. "The Catalytic Oxidation of Micromolar Aqueous Sulphur Dioxide," *Atmos. Environ.* 8:937–945 (1974).
27. Chen, T.I., and C.H. Barron. "Some Aspects of the Homogeneous Kinetics of Sulfite Oxidation," *Ind. Eng. Chem. Fundam.* 11:466–470 (1972).
28. Coughanowr, D.R., and F.E. Krause. "The Reaction of SO_2 and O_2 in Aqueous Solutions of $MnSO_4$," *Ind. Eng. Chem. Fundam.* 4:61–66 (1965).
29. Davies, R., A.K.E. Hagopian and A.G. Sykes. "Kinetics and Oxygen-18 Tracer Studies of Sulphite with the Superoxo Complex $(NH_3)_5Co{\cdot}O_2{\cdot}Co(NH_3)_5^{5+}$ in Aqueous Media," *J. Chem. Soc.* (A):623–629 (1969).
30. Freiberg, J. "The Mechanism of Iron Catalyzed Oxidation of SO_2 in Oxygenated Solutions," *Atmos. Environ.* 9:661–672 (1975).
31. Fuller, E.C., and R.H. Crist. "The Rate of Oxidation of Sulfite Ions by Oxygen," *J. Am. Chem. Soc.* 63:1644–1650 (1941).
32. Linek, V., and J. Mayrhoferova. "The Kinetics of Oxidation of Aqueous Sodium Sulfite Solution," *Chem. Eng. Sci.* 25:787–800 (1970).
33. Matteson, J.J., W. Stöber and H. Luther. "Kinetics of the Oxidation of Sulfur Dioxide by Aerosols of Manganese Sulfate," *Ind. Eng. Chem. Fundam.* 8:677–684 (1969).
34. Sawicki, J.E., and C.H. Barron. "On the Kinetics of Sulfite Oxidation in Heterogeneous Systems," *Chem. Eng. J.* 5:153–159 (1973).
35. Yagi, S., and H. Inoue. "The Adsorption of Oxygen into Sodium Sulfite Solution," *Chem. Eng. Sci.* 17:411–421 (1962).
36. Hoffmann, M.R., and S.D. Boyce. "Theoretical and Experimental Considerations of the Catalytic Autoxidation of Aqueous Sulfur Dioxide in Relationship to Atmospheric Systems," in *Advances in Environmental Science and Technology, Vol. 12,* S.E. Schwartz, Ed. (New York: John Wiley & Sons, Inc., 1982).
37. Backström, H. "Der Kettenmechanisms bei der Autoxydation von Naturimsulfirlösungen," *Z. Phys. Chem.* 25B:122–138 (1934).
38. Bassett, H., and W.G. Parker. "The Oxidation of Sulphurous Acid," *J. Chem. Soc.* (1951), pp. 1540–1560.
39. Lunak, S., and J. Veprek-Siska. "Photochemical Autooxidation of Sulphite Catalyzed by Iron(III) Ions," *Collect. Czech. Chem. Commun.* 41:3495–3503 (1976).
40. Schmittkunz, H. "Chemilumineszenzder Sulfitooxidation," Dissertation, Naturwissenschaftliche Fakultät der Universität Frankfurt, Frankfurt, Germany (1963).
41. Spiro, T. G., Ed. *Metal Ion Activation of Dioxygen* (New York: John Wiley & Sons, Inc., 1980).
42. Walling, C. "Fenton's Reagent Revisited," *Accts. Chem. Res.* 12:125–131 (1975).
43. Lunde, G., J. Gether, N. Gjos and M.S. Lande. "Organic Micropollutants in Precipitation over Norway," *Atmos. Environ.* 11:1007–1014 (1977).

44. Inoue, H., Y. Kida, and E. Imoto. "Organic Catalysts. V. Specific Catalytic Properties of Copper-Iron-Phthalocyanine in the Oxidation of Aldehydes," *Bull. Chem. Soc. Japan* 41:692–696 (1968).
45. Ohkatsu, Y., O. Sekiguchi and T. Osa. "The Liquid-Phase Oxidation of Aldehydes with Fe, Cu-Polyphthalocyanine and Cobalt Tetra-p-tolyporphyrin," *Bull. Chem. Soc. Japan* 50:701–705 (1977).
46. Kothari, V.M., and J.J. Tazuma. "Selective Autoxidation of Some Phenols Using Salcomines and Metal Phthalocyanines," *J. Catal.* 41:180–189 (1976).
47. Tada, M., and T. Katsu. "The Autoxidation of Phenols Catalyzed by Phthalocyanine-Fe(II) and Salcomine-pyridine," *Bull. Chem. Soc. Japan* 45:2558–2559 (1972).
48. Mass, T.A.M.M., M. Kuijer and J. Zwart. "Activation of Cobalt-Phthalocyanine Catalyst by Polymer Attachment," *Chem. Commun.* (1976), pp. 86–88.
49. Wagnerova, D.M., E. Schwertnerova and J. Veprek-Siska. "Autoxidation of Hydrazine Catalyzed by Tetrasulphophthalocyanines," *Collect. Czech. Chem. Commun.* 38:756–764 (1973).
50. Wagnerova, D.M., E. Schwertnerova and J. Veprek-Siska. "Autoxidation of Hydroxylamine Catalyzed by Cobalt(II) Tetrasulphophthalocyanine Models of Oxidases," *Collect. Czech. Chem. Commun.* 39:3036–3047 (1974).
51. Hoffmann, M.R., and B.C. Lim. "Kinetics and Mechanisms of the Oxidation of Sulfite by Oxygen: Catalysis by Homogeneous Metal-Phthalocyanine Complexes," *Environ. Sci. Technol.* 13:1406–1414 (1979).
52. Boucher, L.J. "Metal Complexes of Phthalocyanines," in *Coordination Chemistry of Macrocyclic Compounds,* G.A. Melson, Ed. (New York: Plenum Press, 1979), pp. 461–516.
53. Weber, J.H., and D.H. Busch. "Complexes Derived from Strong Field Ligands. XIX. Magnetic Properties of Transition Metal Derivatives of 4,4,',4",4' "–Tetrasulfophthalocyanine," *Inorg. Chem.* 4:469–470 (1965).
54. Allum, K.G., R.D. Hancock, I.V. Howell, S. McKenzie, R.C. Pitkethly and P.J. Robinson. "Supported Transition Metal Complexes," *J. Organomet. Chem.* 87:203–216 (1975).
55. Leal, O., D.L. Anderson, R.G. Bowman, F. Basolo and R.L. Burwell, Jr. "Reversible Adsorption of Oxygen on Silica Gel Modified by Imidazole-Attached Iron Tetraphenylporphyrin," *J. Am. Chem. Soc.* 97:5125–5129 (1975).
56. Huss, A., Jr., P.K. Lim and C.A. Eckert. "On the Uncatalyzed Oxidation of Sulfur(IV) in Aqueous Solution," *J. Am. Chem. Soc.* 100:6252–6253 (1978).
57. Smith, R.M., and A.E. Martell. *Critical Stability Constants, Vol. 4, Inorganic Complexes* (New York: Plenum Press, 1976).
58. Baldwin, M.E. "Sulphitobis(ethylenediamine) Cobalt(III) Complexes," *J. Chem. Soc.* (1961), pp. 3123–3128.
59. Elder, R.C., M.J. Heeg, M.D. Payne, M. Tikula and E. Deutsch. "Trans Effect in Octahedral Complexes. 3. Comparison of Kinetic and Trans Effects Induced by Coordinated Sulfur in Sulfito- and Sulfinapentamine Cobalt(III) Complexes," *Inorg. Chem.* 17:431–440 (1978).
60. Johansson, L. G., and O. Lindqvist. "Manganese(II) Sulfite Trihydrate," *Acta Crystallog.* B36:2739–2741 (1980).
61. Johansson, L.G., and E. Ljundstrom. "Structure of Iron(II) Sulfite 2.5 Hydrate," *Acta Crystallog.* B36:1184–1186 (1980).
62. Magnusson, A., L.G. Johannson and O. Lindqvist. "The Structure of Manganese(II) Sulfite," *Acta Crystallog.* B37:1108–1110 (1981).

63. Newman, G., and D.B. Powell. "The Infra-red Spectra and Structures of Metal-Sulfite Compounds," *Spectrochim. Acta* 19:213–224 (1963).
64. Raston, C.L., A.H. White and J.K. Yandell. "Structural and Kinetic Effects in Cobalt(III) Complexes with Cobalt-Sulfur Bonds. The Crystal Structure of trans-Bis (Ethylenediamine)-imidazolesulfito-Cobalt(III) Perchlorate Dihydrate," *Aust. J. Chem.* 31:993–998 (1978).
65. Hansen, L.D., L. Whiting, D.J. Eatough, T.E. Jensen and R.M. Izatt. "Determination of Sulfur(IV) and Sulfate in Aerosols by Thermometric Methods," *Anal. Chem.* 48:634–638 (1976).
66. Carlyle, D. "A Kinetic Study of the Aquation of Sulfitoiron(III) Ion," *Inorg. Chem.* 10:761–764 (1974).
67. Hoffmann, M.R., R.A. Stern, P.H. Rieger and J.O. Edwards. "A Kinetic Study of Pyrophosphate and Peroxodiphosphate Complexation of Oxovanadium(IV) Ion," *Inorg. Chim. Acta* 19:181–187 (1976).
68. Abel, E.W., J.M. Pratt and R. Whelan. "Formation of a 1:1 Oxygen Adduct with Cobalt(II)-tetrasulphophthalocyanine," *Chem. Commun.* (1971), pp. 449–450.
69. Veprek-Siska, J., E. Schwertnerova and D.M. Wagnerova. "Reversible Reaction of Cobalt(II) Tetrasulfophthalocyanine with Molecular Oxygen," *Chimia* 26:75–76 (1972).
70. Bernauer, K., and S. Fallab. "Phthalocyanine in wässeriger Lösung I," *Helv. Chim. Acta* 44:1287–1292 (1961).
71. Gruen, L.C., and R.J. Blagrove. "The Aggregation and Reaction of the Tetrasodium Salt of Cobalt Phthalocyanine-4,4′,4″,4′ ″-Tetrasulphonic Acid," *Aust. J. Chem.* 26:319–323 (1973).
72. Schelly, Z.A., R.D. Farina and E.M. Eyring. "A Concentration-Jump Relaxation Method Study on the Kinetics of the Dimerization of the Tetrasodium Salt of Aqueous Cobalt(II)-4,4′,4″,4′ ″-Tetrasulfophthalocyanine," *J. Phys. Chem.* 74:617–620 (1970).
73. Rollman, L.D., and R.T. Iwamoto. "Electrochemistry, Electron Paramagnetic Resonance and Visible Spectra of Cobalt, Nickel, Copper and Metal-Free Phthalocyanines in Dimethyl Sulfoxide," *J. Am. Chem. Soc.* 90:1455–1463 (1968).
74. Kropf, H. "Catalysis by Phthalocyanine Complexes," *Angnew. Chem. Int. Ed.* 11:239–240 (1972).
75. Kropf, H., and H.D. Hoffmann. "Autoxidation von Cumol in Gegenwart von Substituierten Kupfer-Phthalocyaninen und Verwandten Kupfer-Komiplexen," *Tetrahedron Lett.* (1967), pp. 659–663.
76. Basolo, F., B.M. Hoffmann and J.A. Ibers. "Synthetic Oxygen Carriers of Biological Interest," *Accts. Chem. Res.* 8:384–392 (1975).
77. Jones, R.D., D.A. Summerville and F. Basolo. "Synthetic Oxygen Carriers Related to Biological Systems," *Chem. Rev.* 79:139–179 (1979).
78. Collmann, J.P., T.R. Halbert and K.S. Suslick. "O_2 Binding to Hemes and Their Synthetic Analogs," in *Metal Ion Activation of Dioxygen,* T.G. Spiro, Ed. (New York: John Wiley & Sons, Inc., 1980), pp. 1–72.
79. McLendon, G., and A.E. Martell. "Inorganic Oxygen Carriers as Models for Biological Systems," *Coord. Chem. Rev.* 19:1–39 (1976).
80. Sigel, H., P. Waldmeier and B. Prijs. "The Dimerization, Polymerization, and Hydrolysis of Fe^{III}-4,4′,4″,4′ ″-Tetrasulfophthalocyanine," *Inorg. Nucl. Chem. Lett.* 7:161–169 (1971).
81. Vonderschmitt, D., K. Bernauer and S. Fallab. "Reaktivat von Koordinationverbin-

dungen XIV [1]. Reversible O_2-Bindung an Eisen(II)-Phthalocyanintetrasulfonsäure," *Helv. Chim. Acta* 48:951–954 (1964).

82. Wagnerova, D.M., E. Schwertnerova and J. Veprek-Siska. "Kinetics of the Reaction of Cobalt(II) Tetrasulphophthalocyanine with Molecular Oxygen," *Collect. Czech. Chem. Commun.* 39:1980–1988 (1974).
83. Cook, A.H. "Catalytic Properties of the Phthalocyanines. Part I. Catalase Properties," *J. Chem. Soc.* (1938), pp. 1761–1768.
84. Cook, A.H. "Catalytic Properties of the Phthalocyanines. Part II. Oxidase Properties," *J. Chem. Soc.* (1938), pp. 1768–1774.
85. Cook, A.H. "Catalytic Properties of the Phthalocyanines. Part III," *J. Chem. Soc.* (1938), pp. 1774–1780.
86. Dolansky, J., D.M. Wagnerova and J. Veprek-Siska. "Autoxidation of Cysteine Catalyzed by Cobalt(II) Tetrasulphophthalocyanine. Models of Oxidases V," *Collect. Czech. Chem. Commun.* 41:2326–2332 (1976).
87. Laidler, K., and P.S. Bunting. *The Chemical Kinetics of Enzyme Action* (Oxford: Clarendon Press, 1973).
88. King, E.L., and C. Altman. "A Schematic Method of Deriving the Rate Laws for Enzyme Catalyzed Reactions," *J. Phys. Chem.* 60:1375–1378 (1956).
89. Schutten, J.H., and T.P.M. Beelen. "The Role of Hydrogen Peroxide During the Autoxidation of Thiols Promoted by Bifunctional Polymer-Bonded Cobalt Phthalocyanine Catalysts," *J. Molec. Catal.* 10:85–97 (1981).
90. Holt, B.D., R. Kumar and P.T. Cunningham. "Oxygen-18 Study of the Aqueous Phase Oxidation of Sulfur Dioxide," *Atmos. Environ.* 15:557–566 (1981).
91. Yatsimirskii, K., B. Bratushko, I. Yu and I.L. Zatsny. "Kinetics and Mechanism of the Reduction of Molecular Oxygen Coordinated in the Complex Co_2(L-histidine)$_4O_2$ by Sodium Sulphite in Aqueous Solution," *Zh. Neorgh. Khimii* 22:1611–1616 (1977).
92. Beelen, T.P.M., C.O. de Costa Gomez and M. Kuijer. "The Enhancement by Visible Light of the Catalytic Activity of Co(II)-Tetrasulphophthalocyanine on the Oxidation of Mercapto-Ethanol," *Recl. Trav. Chim. Pays-Bas.* 98:521–522 (1979).
93. Cox, G.S., D.G. Whitten and C. Giannotti. "Interaction of Porphyrin and Metalloporphyrin Excited States with Molecular Oxygen. Energy-Transfer Quenching Mechanisms in Photo Oxidations," *Chem. Phys. Lett.* 67:511–515 (1979).
94. Frost, A.A., and R.G. Pearson. *Kinetics and Mechanism* (New York: John Wiley & Sons, Inc., 1961).
95. Cookson, D.J., T.D. Smith, J.F. Boas, P.R. Hicks and J.R. Pilbrow. "Electron Spin Resonance Study of the Autoxidation of Hydrazine, Hydroxylamine and Cysteine Catalyzed by the Cobalt(II) Chelate Complex of 3,10,17,24-Tetrasulphophthalocyanine," *J. Chem. Soc.* (1977), pp. 109–114.
96. Theorell, H., and B. Chance. "Studies on Liver Alcohol Dehydrogenase. II. The Kinetics of the Compound of Horse Liver Alcohol Dehydrogenase and Reduced Diphosphopyridine Nucleotide," *Acta Chem. Scand.* 5:1127–1144 (1951).
97. Liu, B.Y.H., D.Y.H. Pui, K.T. Whitby and D.B. Kittelson. "The Aerosol Mobility Chromatograph: A New Detector for Sulfuric Acid Aerosols," *J. Aerosol Sci.* 6:433–451 (1978).
98. McMurry, P.H., and B.Y.H. Liu. "The Tandem Differential Mobility Analyzer Applied to Studies on Particle Growth and Gas Phase Titration," DOE Report EY-76-S-02-1248 (1978).
99. Schwartz, S.E. and J.E. Freiberg. "Mass-Transport Limitation to the Rate of Reaction

of Gases in Liquid Droplets: Application to Oxidation of SO_2 in Aqueous Solutions," *Atmos. Environ.* 15:1129–1144 (1981).

100. Freiberg, J.E., and S.E. Schwartz. "Oxidation of SO_2 in Aqueous Droplets: Mass-Transport Limitation in Laboratory Studies and the Ambient Atmosphere," *Atmos. Environ.* 15:1145–1154 (1981).
101. Schutten, J.H., P. Piet and A.L. German. "Some Observations on Complexes of a Cobalt Phthalocyanine with Poly(vinylamine) and Their Catalytic Activity in the Autoxidation of Thiols," *Makromol. Chem.* 180:2341–2350 (1979).
102. Schutten, J.H., and J. Zwart. "Autoxidation of Mercaptans Promoted by a Bifunctional Catalyst Prepared by Polymer Attachment of Cobalt-Phthalocyanine," *J. Mol. Catal.* 5:109–123 (1979).
103. Schutten, J.H., C.H. van Hastenberg, P. Piet and A.L. German. "Marcroporous Styrene Divinylbenzene Copolymers for Poly(vinylamine)–Cobaltphthalocyanine Oxidation Catalysts," *Angew. Makromol. Chem.* 89:201–219 (1980).
104. McCord, J.M., and I. Fridovich. "The Utility of Superoxide Dismutase in Studying Free Radical Reactions," *J. Biol. Chem.* 244:6056–6063 (1969).
105. Cohen, S.H., S.G. Chang, S.S. Markowitz and T. Novakov. "Role of Fly Ash in Catalytic Oxidation of S(IV) Slurries," *Environ. Sci. Technol.* 15:1498–1502 (1981).
106. Kok, G.L. "Measurements of Hydrogen Peroxide in Rainwater," *Atmos. Environ.* 14:653–656 (1980).
107. Kok, G.L. "Measurements of Hydrogen Peroxide in Rainwater," *EOS Trans. Am. Geophys. Union* 45:884 (1981).